Entamoeba histolytica develops resistance to complement deposition and lysis after acquisition of human complement regulatory proteins through trogocytosis

Hannah W. Miller[1], Tammie S.Y. Tam[1] and Katherine S. Ralston[1*]

[1]Department of Microbiology and Molecular Genetics, University of California, Davis, USA

[*]Address correspondence to Katherine S. Ralston, ksralston@ucdavis.edu

Running Title: Evasion of complement lysis by *Entamoeba histolytica*

ABSTRACT

Entamoeba histolytica is the cause of amoebiasis. The trophozoite (amoeba) form of this parasite is capable of invading the intestine, and can disseminate through the bloodstream to other organs. The mechanisms that allow amoebae to evade complement deposition during dissemination have not been well characterized. We previously discovered a novel complement-evasion mechanism employed by *E. histolytica*. *E. histolytica* ingests small bites of living human cells in a process termed trogocytosis. We demonstrated that amoebae were protected from lysis by human serum following trogocytosis of human cells, and that amoebae acquired and displayed human membrane proteins from the cells they ingested. Here, we aimed to define how amoebae are protected from complement lysis after performing trogocytosis. We found that amoebae were protected from complement lysis after ingestion of both human Jurkat T cells and red blood cells, and that the level of protection correlated with the amount of material ingested. Trogocytosis of human cells led to a reduction in deposition of C3b on the surface of amoebae. We asked whether display of human complement regulators is involved in amoebic protection, and found that CD59 was displayed by amoebae after trogocytosis. Deletion of a single complement regulatory protein, CD59 or CD46, from Jurkat cells was not sufficient to alter amoebic protection. Removal of all GPI-anchored proteins, including CD59 and CD55, from the surface of amoebae that had undergone trogocytosis suggested that multiple, redundant complement regulators mediate amoebic protection. These studies shed light on a novel strategy for immune evasion by a pathogen.

19 **IMPORTANCE**

20 *Entamoeba histolytica* is the cause of amoebiasis, a diarrheal disease of global importance. While
21 infection is often asymptomatic, the trophozoite (amoeba) form of this parasite is capable of invading and
22 ulcerating the intestine, and can disseminate through the bloodstream to other organs. Understanding how *E.*
23 *histolytica* evades the complement system during dissemination is of great interest. Here we demonstrate for
24 the first time that amoebae that have performed trogocytosis (nibbling of human cells) resist deposition of the
25 complement protein C3b. Amoebae that have performed trogocytosis display the complement regulatory
26 protein CD59. Overall, our studies suggest that acquisition and display of multiple, redundant complement
27 regulators is involved in amoebic protection from complement lysis. These findings shed light on a novel
28 strategy for immune evasion by a pathogen. Since other parasites use trogocytosis for cell killing, our findings
29 may apply to the pathogenesis of other infections.

30 **INTRODUCTION**

31 Amoebiasis remains a disease of global importance. The 2015 Global Burden of Disease Study
32 estimated that it was responsible for 67,900 deaths worldwide that year (1). Its causative agent, *Entamoeba*
33 *histolytica,* is prevalent in countries with poor sanitation and is spread through feces-contaminated food and
34 water (2). In the rural area of Durango, Mexico, the seroprevalence of *E. histolytica* was found to be as high as
35 42% (3), and a longitudinal study of children living in an urban community of Dhaka, Bangladesh found that
36 80% were infected with the parasite by two years of age (4).

37 While infection with *E. histolytica* is often asymptomatic, it can result in diarrheal disease, colitis and
38 extraintestinal abscesses (5). Following ingestion of the cyst form of the parasite, excystation occurs and the
39 trophozoite stage (amoeba) colonizes the large intestine (6). Amoebae are capable of invading and ulcerating
40 the intestine, causing tissue damage and bloody diarrhea. They can also disseminate through the bloodstream
41 to other organs, most commonly the liver, where they form abscesses that are fatal if left untreated (5). The
42 mechanisms that allow amoebae to evade complement deposition during dissemination have not been well
43 characterized. Pathogenic strains of *E. histolytica* isolated from patients have been shown to be more resistant
44 to complement lysis than nonpathogenic strains (7). It has also been found that the pathogenic amoeba
45 species *E. histolytica* appears to be more resistant to complement than its nonpathogenic relative *E. dispar* (8).
46 *E. histolytica* cysteine proteases can cleave complement components (9–11), and the Gal/GalNAc lectin has
47 been described as a CD59 mimicry molecule (12). However, these mechanisms alone are not sufficient to fully
48 protect amoebae from complement lysis, as trophozoites are readily lysed by human serum *in vitro* (13).

49 We previously discovered a novel complement-evasion mechanism employed by *E. histolytica* (13).
50 Trogocytosis, or "cell nibbling," is present in many eukaryotes and occurs in a variety of contexts (14). In *E.*
51 *histolytica*, trogocytosis is a process in which amoebae ingest small bites of living human cells (15). Our
52 previous work has defined amoebic trogocytosis as both a mechanism for cell killing (15), and more recently,
53 for immune evasion (13). We demonstrated that amoebae were protected from lysis by human serum

following trogocytosis of human cells (13), and that amoebae acquired and displayed human membrane proteins from the cells they ingested (13). This work suggested a model in which amoebae incorporate proteins from human cells they eat on their surface, and these proteins in turn inhibit complement lysis.

In the present study, we aimed to define the mechanism by which amoebae are protected from complement lysis after performing trogocytosis. We found that trogocytosis of human cells reduced deposition of the complement protein C3b the surface of amoebae, and that amoebae were protected from complement lysis after ingestion of both human Jurkat T cells and primary red blood cells. We identified the human complement regulatory protein CD59 (protectin) as one of the proteins that is taken from ingested human cells and displayed on the amoebic surface. Deletion of a single complement regulatory protein, CD59 or CD46, from human Jurkat cells was not sufficient to alter conferred protection on amoebae. Overall, these studies suggest that multiple, redundant complement regulators are involved in amoebic protection.

65 **RESULTS**

66 **Amoebic protection from complement following trogocytosis is dose-dependent.**

67 To determine if the amount of trogocytosed human cell material influenced protection, or if any level
68 of trogocytosis was protective, we allowed amoebae to ingest incrementally larger amounts. Amoebae
69 became increasingly protected from complement lysis **(Fig. 1b-c, S3a)** after ingesting higher quantities of live
70 Jurkat cell material **(Fig. 1a, 1g)**. Thus, acquired protection from complement lysis correlates with the amount
71 of human cell material ingested through trogocytosis.

72 We next asked if protection could be conferred through trogocytosis of primary human cells. During
73 invasive infections, amoebae breach the intestinal wall and disseminate via the bloodstream. Detection of
74 amoebae containing ingested red blood cells in the stool has previously been used as a diagnostic for invasive
75 disease (16). Therefore, we asked if ingestion of human red blood cells would lead to protection. Amoebae
76 were allowed to ingest increasing numbers of human red blood cells. Increased trogocytosis of red blood cells
77 led to increased protection from complement lysis **(Fig. 1d-f, 1h, S3b)**. These results support a model where
78 the level of protection from complement lysis is proportional to the amount of human cell material that was
79 ingested during trogocytosis.

80 **Amoebic trogocytosis of human cells inhibits deposition of complement C3b.**

81 It can be inferred that lysis of amoebae by human serum is due to complement activity because heat-
82 inactivated serum does not lyse amoebae (13). Here, we formally tested if trogocytosis of human cells led to
83 reduced deposition of complement on the amoebae surface. Amoebae that had been co-incubated with live
84 human cells had less death and less deposited human C3b on their surface than amoebae that were incubated
85 alone **(Fig. 2 a-b, S4)**. Furthermore, live amoebae had less deposited C3b than dead amoebae **(Fig. 2c, 2e)**.
86 Among amoebae had been co-incubated with human cells, both live and dead amoebae had less deposited
87 C3b, compared to amoebae that were incubated alone **(Fig. 2d)**. Therefore, trogocytosis of human cells
88 prevents complement lysis of amoebae and inhibits deposition of complement C3b.

Amoebae acquire the complement regulatory protein CD59 from human cells.

We hypothesized that protection from complement lysis was due to display of human complement regulatory proteins. We first chose to look at acquisition of the complement regulatory protein CD59 (protectin), a membrane protein that is expressed by both Jurkat cells and human red blood cells (17–19). CD59 inhibits terminal components of the complement cascade and formation of the membrane attack complex (17, 20–22). After amoebae had performed trogocytosis, patches of CD59 were detected on the amoeba surface within five minutes **(Fig. 3a)** and a larger quantity of CD59 patches were detected on the amoeba surface after one hour of trogocytosis **(Fig. 3a-c)**. The patchy/punctate localization pattern is similar to the localization pattern of other human proteins displayed by amoebae after trogocytosis (13). Since the heavy chain of the amoeba surface Gal/GalNAc lectin has been implicated as a CD59 mimicry molecule (12, 23), we asked if the CD59 antibody used in these assays cross-reacted with the Gal/GalNAc lectin. Importantly, we did not see CD59 labeling on control amoebae that had not performed trogocytosis **(Fig. 3a**), showing that the CD59 antibody did not cross-react with the Gal/GalNAc lectin.

Imaging flow cytometry analysis was used to quantify amoebic acquisition of CD59. Human cell nuclei are not ingested during trogocytosis (15). Therefore, labeling of human cell nuclei was used to differentiate intact, extracellular human cells from patches of human proteins displayed on amoebae. Patches of displayed human CD59 were detected on amoebae that had performed trogocytosis, but not on amoebae that were incubated alone **(Fig. 4a-c, S5)**. Amoebae had ~38% more displayed CD59 after one hour of trogocytosis than after five minutes **(Fig. 4b)**. These findings indicate that amoebae acquired and displayed CD59 within five minutes of trogocytosis, and the quantity of displayed CD59 increased over time.

Removal of GPI-anchored surface proteins trends towards restoring complement lysis of amoebae.

We next sought to test the effect of removing complement regulatory proteins on conferred protection. CD59 is a glycosylphosphatidylinositol (GPI) anchored protein that can be cleaved with the enzyme phosphatidylinositol-specific phospholipase C (PI-PLC) (17, 18, 20, 22). In addition to removing CD59,

13 treatment with PI-PLC also cleaves the GPI-anchored complement regulatory protein CD55 (Decay-
14 accelerating factor) (24, 25). CD55 is expressed by both Jurkat cells and human red blood cells (19, 26) and
15 accelerates the decay of C3 and C5 convertases of the classical and alternative complement pathways (26, 27).
16 Amoebae were allowed to perform trogocytosis or incubated alone, and then treated with PI-PLC before
17 exposure to human serum. Heat-inactivated PI-PLC was used as a control. PI-PLC treatment appeared to
18 reduce amoebic protection from complement lysis **(Fig. S1a, S6)**. However, this difference was not statistically
19 significant. This is likely to be due to the higher levels of variability in this assay, which were due to the
20 prolonged incubation of amoebae on ice during PI-PLC treatment. Indeed, due to the incubation on ice, the
21 background level of cell death of untreated amoebae was much higher than typical. These findings suggested
22 that removal of all GPI-anchored proteins reduces amoebic protection from complement lysis, but did not
23 prove a causal relationship.

24 **Removal of CD59 and CD46 is not sufficient to sensitize amoebae to complement lysis.**

25 Due to the higher levels of variability that we observed with PI-PLC treatment, we next used human cell
26 mutants to test whether individual proteins were required for protection from complement lysis. We tested
27 the requirements for CD59 and CD46. CD46 (Membrane cofactor protein) is expressed by human Jurkat cells
28 (28) and acts as a co-factor for serum factor I, which cleaves and inactivates complement components C3b and
29 C4b (29–31). In order to determine if acquisition and display of human CD59 or CD46 molecules was required
30 for protection from complement, we used CRISPR/Cas9 to create human cell knockout mutants that lacked
31 these proteins. Sanger sequencing **(Fig. S2)** and antibody staining of CD59 **(Fig. 5a-b)** and CD46 **(Fig. 5c-d)**
32 showed that knockout mutants were successfully generated. Amoebae that were allowed to perform
33 trogocytosis on control human cells or cells that lacked either CD59 or CD46 were equally protected from
34 complement lysis **(Fig. 5e, S6)**. Additionally, there was no difference in the amount of ingested human cell
35 material **(Fig. 5f)**. These findings reveal that removal of either CD59 or CD46 individually is not sufficient to
36 sensitize amoebae to complement lysis. Furthermore, they hint at redundancy in the mechanism of protection

and that amoebae likely acquire and display multiple complement regulatory proteins from the cells they ingest.

39 **DISCUSSION**

40 Our findings reveal that amoebae are protected from complement lysis through trogocytosis of human
41 cells and that ingestion of human cells leads to less deposited C3b on the amoeba surface. Amoebae acquire
42 protection from both human Jurkat cells as well as primary red blood cells and conferred protection is
43 proportional to the amount of ingested human cell material. Trogocytosis of human cells results in the display
44 of the complement regulatory protein CD59 on the amoebae surface. Finally, although removal of the
45 individual complement regulatory proteins CD59 and CD46 did not influence acquired protection, removal of
46 all GPI anchored proteins, including CD59 and CD55, was associated with a non-significant loss in acquired
47 protection.

48 Many studies have shown that cancer cells overexpress complement regulatory molecules, allowing
49 them to evade complement lysis. However, it should be noted that expression levels vary widely between cell
50 types and between individual studies (32). Removal of GPI-anchored proteins, which include the complement
51 regulatory proteins CD59 and CD55 but not CD46, with PI-PLC treatment resulted in enhanced susceptibility of
52 cancer cells to complement lysis (24, 25). This is consistent with our finding that PI-PLC treated amoebae that
53 had undergone trogocytosis of human cells, and been made resistant to complement, became more sensitive
54 to complement lysis. Treatment with PI-PLC removes other GPI-anchored proteins in addition to CD59 and
55 CD55, so we cannot rule out the possibility that loss of other membrane proteins contributed to the loss of
56 complement resistance in our PI-PLC treated amoebae.

57 There have been several studies that examined the efficacy of using blocking antibodies against
58 complement regulatory proteins to enhance lysis of cancer cells. Results from blocking individual proteins
59 have been highly variable in different cell types but blocking one or more proteins was effective in many cases.
60 Using antibodies against CD46 was rarely effective, however antibodies against CD59 and CD55 often were
61 effective in enhancing complement lysis (32). Additionally, there appears to be an additive effect when
62 multiple proteins are targeted at once. Cervical carcinoma cells were rendered more susceptible to

53 complement after treatment with blocking antibodies to CD59 and CD55, and lysis was increased further when
54 cells were treated with both antibodies (33). Similarly, breast carcinoma cells, were more easily lysed after
55 treatment with anti-CD59 and anti-CD55 antibodies, but a much higher degree of lysis was achieved when a
56 mixture of anti-CD59, anti-CD55, and anti-CD46 antibodies was used (34). Since neither removal of CD46 or
57 CD59 was sufficient to sensitize amoebae to complement lysis, it is possible that amoebic display of multiple
58 different complement regulators enables protection from lysis. While removal of CD46 or CD59 did not
59 sensitize amoebae to complement lysis, these proteins could still contribute to amoebic complement
70 protection, as part of a collection of multiple redundant, complement regulators that protect amoebae from
71 lysis. Since we found that amoebae that have performed trogocytosis are resistant to C3b deposition, it is
72 possible that multiple complement regulators that act earlier in the complement cascade, upstream of C3b
73 deposition, are needed for protection from complement lysis.

74 Our results support a model whereby amoebae are protected from serum lysis in the blood through
75 trogocytosis of red blood cells they encounter there, and potentially from other cells they encounter before
76 reaching the bloodstream. Amoebae likely acquire and display multiple complement regulatory proteins from
77 the human cells that they ingest, which then leads to less C3b deposition, and protection from complement
78 lysis.

79 **MATERIALS AND METHODS**

80 **Cell culture**

81 *E. histolytica* trophozoites (HM1:IMSS) from ATCC (amoebae) were cultured as described previously
82 (13). Amoebae were maintained in glass tissue culture tubes at 35°C in TYI-S-33 medium supplemented with
83 15% heat-inactivated adult bovine serum (Gemini Bio-Products), 2.3% Diamond vitamin Tween 80 solution
84 (40×; Sigma-Aldrich), and 80 U/ml penicillin, 80 µg/ml streptomycin (Gibco). Amoebae were expanded in T25
85 un-vented tissue culture flasks and harvested when flasks reached 80% confluence. When used in serum lysis
86 or immunofluorescence assays, amoebae were resuspended in M199s medium (Gibco medium M199 with
87 Earle's salts, L-glutamine, and 2.2 g/liter sodium bicarbonate, without phenol red) supplemented with 0.5%
88 bovine serum albumin (BSA), 25 mM HEPES, and 5.7 mM L-cysteine.

89 Human Jurkat T cells (clone E6-1) from ATCC were grown in vented T25 tissue culture flasks at 37°C and
90 5% CO2 as previously described (13). Jurkat cells were cultured in RPMI 1640 medium (Gibco; RPMI 1640 with
91 L-glutamine and without phenol red) supplemented with 10% heat-inactivated fetal bovine serum (Gibco), 100
92 U/ml penicillin, 100 µg/ml streptomycin, and 10 mM HEPES. Jurkat cells were expanded in T75 vented tissue
93 culture flasks and harvested when cell density reached between 5×10^5 and 2×10^6 cells/ml. Jurkat cells were
94 resuspended in M199s medium for use in serum lysis or immunofluorescence assays.

95 Single donor human red blood cells separated from whole blood by centrifugation and negative for the
96 presence of human immunodeficiency virus-1 (HIV-1), HIV-2, HIV-1 antigen or HIV-1 nucleic acid test, hepatitis
97 B surface antigen, hepatitis C virus , syphilis, and alanine aminotransferase test were purchased from
98 Innovative Research (Cat# IWB3CPDA1UNIT). Red blood cells were stored at 4°C and resuspended in M199s
99 medium prior to use in serum lysis assays.

100 **DNA constructs**

101 Guide RNAs (gRNA) to human CD59 or CD46 were cloned into a pX330-U6-Chimeric_BB-CBh-hSpCas9
102 plasmid backbone (pX330-U6-Chimeric_BB-CBh-hSpCas9 was a gift from Feng Zhang (Addgene plasmid #

)3 42230; http://n2t.net/addgene:42230 ; RRID:Addgene_42230) (35)). Guide RNAs were created by using the

)4 sequences designed by Thielen et. al, 2018 (36). The gRNA oligos used are presented in **Table 1** with BbsI

)5 restriction enzyme overhangs shown in bold. Guide RNAs were cloned into the pX330-U6-Chimeric_BB-CBh-

)6 hSpCas9 plasmid backbone using a modified version of the Zhang Lab General Cloning Protocol (Addgene

)7 http://www.addgene.org/crispr/zhang/). Briefly, the px330 plasmid backbone was digested with BbsI

)8 restriction enzyme (FastDigest BpiI: ThermoFisher Scientific). Guide RNA oligos containing BbsI overhangs

)9 were then phosphorylated and annealed. Next, annealed oligos were ligated into the pX330 plasmid backbone

10 and NEB 5-alpha Competent *E. coli* were transformed (New England Biolabs). Positive colonies were screened

11 by restriction digest. Plasmids with the correct inserts were confirmed by Sanger sequencing using the "U6"

12 Universal Primer from GENEWIZ (LKO.1 5') which is located in the human U6 promoter **(Table 1)**.

13 **Jurkat T cell CRISPR/Cas9 mutants**

14 Human Jurkat T cells were transfected with pX330 plasmids containing the CD59 gRNA, the CD46

15 gRNA, or the pX330 backbone as a control. Plasmid DNA was isolated in an endotoxin-free manner (GenElute™

16 HP Endotoxin-Free Plasmid Maxiprep Kit; Sigma-Aldrich) and concentrated using paramagnetic beads

17 (HighPrep PCR Clean Up System; Magbio). Jurkat T cells were transfected using the Neon Transfection System

18 (Invitrogen) with the 10 µl tip and 24 well plate format. Cells were prepared, and the Neon Transfection

19 System was used according to the manufacturer's instructions. The transfection conditions used were as

20 follows: volts = 1050, width = 30 and pulse # = 2.

21 When creating the CD59 and CD46 knockout mutants, 1.8 µg of plasmid DNA was used with 1 x 10^5

22 cells per transfection reaction and two reactions were performed for each plasmid and transferred to 1 well of

23 a 24 well plate. Transfection efficiency was calculated by separately transfecting an enhanced green

24 fluorescent protein (EGFP) expression plasmid pcDNA3-EGFP (pcDNA3-EGFP was a gift from Doug Golenbock

25 (Addgene plasmid # 13031 ; http://n2t.net/addgene:13031 ; RRID:Addgene_13031)) in parallel. Percentage of

26 EGFP expressing cells was calculated after 24 hours by fixing samples with 4% paraformaldehyde (Electron

27 Microscopy Sciences) and analyzing with imaging flow cytometry. To generate CD59 expressing Jurkat cells, 2
28 µg of plasmid DNA was used with 2 x 10^5 cells per transfection reaction and two reactions were performed for
29 each plasmid and transferred to 1 well of a 24 well plate.

30 Clonal lines of Jurkat cell mutants were obtained by limiting dilution in 96 well plates. Clonal lines were
31 screened for knockout by labeling with primary mouse monoclonal antibodies to CD59 (clone MEM-43/5;
32 Abcam) or CD46 (clone C-10; Santa Cruz Biotechnology) and a Cy™5 AffiniPure Goat Anti-Mouse secondary
33 antibody (Jackson ImmunoResearch Laboratories, Inc). Samples were analyzed by imaging flow cytometry.
34 Knockout was confirmed in positive clones by isolating genomic DNA using the Quick-DNA Miniprep kit (Zymo
35 Research) and polymerase chain reaction (PCR) amplifying regions of either CD59 or CD46. Primer sets had
36 been identified in BLAST as specific to these genes **(Table 1)**. Next, purified PCR product was sequenced with
37 primers upstream of the predicted CRISPR/Cas9 cut site **(Table 1)** and knockout was confirmed.

38 **Detection of CD59 displayed by amoebae using imaging flow cytometry**

39 Jurkat cells were with labeled Hoechst 33342 dye (Invitrogen) at 5 µg/ml for 30 minutes at 37°C.
40 Amoebae were washed and resuspended in M199s medium and labeled with CellTracker green 5-
41 chloromethylfluorescein diacetate (CMFDA; Invitrogen) at 186 ng/ml for 10 minutes at 35°C. Amoebae and
42 Jurkat cells were then washed and resuspended in M199s medium. Amoebae were resuspended at 4 x 10^5
43 cells/ml and Jurkat cells were resuspended at 1.6 x 10^7 cells/ ml for a 1:40 amoeba: Jurkat cell ratio. Amoebae
44 and Jurkat cells were coincubated for either 5 minutes or 1 hour, or amoebae were incubated alone. Cells
45 were fixed with 4% PFA for 30 minutes at room temperature. Samples were blocked in 1 x PBS containing 0.1%
46 Tween20 (Sigma-Aldrich) (1 x PBST), 5% BSA and 20% Normal Goat Serum (Jackson ImmunoResearch
47 Laboratories, Inc) for 1 hour at room temperature on a rocker. Next, samples were labeled with primary
48 mouse monoclonal antibodies to either CD59 (clone MEM-43/5; Abcam) diluted 1:50 in blocking solution at
49 4°C overnight on a rocker. Samples were washed with 1 x PBST and labeled with a Cy5 AffiniPure Goat Anti-
50 Mouse secondary antibody (Jackson ImmunoResearch Laboratories, Inc) stored in 50% glycerol (Sigma-

51 Aldrich). The secondary antibody was diluted 1:100 in blocking solution, for a final dilution of 1:200, and
52 incubated for 3 hours at room temperature on a rocker. Lastly, samples were washed with 1 x PBST,
53 resuspended in 50 µl 1 x PBS, and run on an Amnis ImageStreamX Mark II. 10,000 events were collected for
54 conditions where amoebae were incubated alone and 100,000 events were collected for conditions where
55 amoebae were incubated with Jurkat cells. Data are from 5 replicates across 3 independent experiments. The
56 no primary control condition was performed in 2 of 3 independent experiments and data are from 3
57 replicates. See Figure S5 for the analysis gating scheme.

58 **Detection of CD59 displayed by amoebae using confocal microscopy**

59 Cells were labeled for confocal microscopy as described previously (13). Amoebae were prepared in
60 the same manner as the for the detection of CD59 using imaging flow cytometry (above) with an approximate
61 fourfold increased concentration of CMFDA. After labeling with antibodies, samples were mounted using
62 Vectashield (Vector Laboratories) on Superfrost Plus microslides (VWR) with glass coverslips. Slides were
63 imaged on an Intelligent Imaging Innovations hybrid Spinning Disk Confocal-TIRF-Widefield Microscope. 136
64 Images were collected from 1 independent experiment. FIJI software was used for image analysis (37).

65 **Serum lysis assays**

66 For experiments where amoebae were incubated with increasing numbers of Jurkat cells, amoebae
67 were washed and resuspended in M199s medium and labeled with CMFDA at 186 ng/ml for 10 minutes at
68 35°C. Jurkat cells were washed and labeled in M199s with DiD at 21 µg/ml for 5 minutes at 37°C and 10
69 minutes at 4°C. Amoebae were washed and resuspended at 4 x 10^5 cells/ml. Jurkat cells were washed a
70 resuspended at 2 x 10^6 cells/ml, 4 x 10^6 cells/ml, 8 x 10^6 cells/ml and 1.6 x 10^7 cells/ml. Amoebae were
71 incubated alone or the presence of Jurkat cells at a 1:5, 1:10, 1:20, and 1:40 ratio for 1 hour at 35°C. Next,
72 samples were resuspended in 100% normal human serum (pooled normal human complement serum;
73 Innovative Research Inc.) supplemented with 150 µM $CaCl_2$ and 150 µM $MgCl_2$ for 30 minutes at 35°C as
74 described previously (13). Following exposure to human serum, samples were resuspended in M199s medium

75 and labeled using Zombie Violet Fixable Viability dye (BioLegend), prepared according to the manufacturer's
76 instructions, at a concentration of 4 µl/ml for 30 minutes on ice. Next, samples were fixed with 4% PFA at
77 room temperature for 30 minutes. Samples were then resuspended in 50 µl 1 x PBS, and run on an Amnis
78 ImageStreamX Mark II. 10,000 events were collected for samples where amoebae were incubated alone or
79 with Jurkat cells at a 1:5 ratio. 10,00 – 20,000 events were collected for samples with Jurkat cells at a 1:10
80 ratio, 10,00 - 40,000 events were collected for samples with a 1:20 ratio, and 50,000 - 80,000 events for
81 samples with a 1:40 ratio. Data are from 6 replicates across 3 independent experiments. See Figure S3 for the
82 analysis gating scheme.

83 For experiments with CD59 and CD46 knockout mutants, the serum lysis assay used was the same as
84 described above, except only a 1:40 ratio of amoebae to Jurkat cells was used, instead of multiple different
85 ratios. Amoebae were incubated alone, in the presences of Jurkat cells transfected with the px330 vector
86 control, or with either CD59 or CD46 knockout Jurkat cell mutants at a 1:40 ratio. Cells were gated on by size
87 and 10,000 events from the amoeba alone conditions and 100,000 events of the amoebae incubated with
88 Jurkat cells conditions were collected. Data are from 6 replicates across 3 independent experiments. See
89 Figure S6 for the analysis gating scheme.

90 In experiments where samples were treated with phospholipase C , the assay was performed as
91 described above with the addition of a treatment step preceding exposure to serum. Only a 1:40 ratio of
92 amoebae to Jurkat cells was used, instead of multiple different ratios. Following coincubation of amoebae and
93 Jurkat cells, samples were immediately placed on ice and resuspended in ice-cold M199s medium. Samples
94 were treated with either 500 mU of Phospholipase C (PI-PLC) (Phospholipase C, Phosphatidylinositol-specific
95 from *Bacillus cereus*; Sigma-Aldrich) prepared according to the manufacturer's instructions, or 500 mU heat-
96 inactivated PI-PLC. PI-PLC was heat-inactivated at 95°C for 30 minutes. PI-PLC was carried out on ice, on a
97 rocker, in a 4°C cold room for 30 minutes. Cells were gated on by size and 10,000 events from the amoebae
98 alone conditions and 100,000 events of the amoebae incubated with Jurkat cells were collected. Data are from

8 replicates across 4 independent experiments. The untreated control condition was performed 3 of 4 independent experiments and data are from 6 replicates. See Figure S6 for the analysis gating scheme.

For experiments where amoebae were incubated with increasing numbers of red blood cells, amoebae were incubated with red blood cells resuspended at 4 x 10^6 cells/ml, 4 x 10^7 cells/ml, and 4 x 10^8 cells/ml for a 1:10, 1:100, and 1:1000 amoebae to red blood cell ratio. The amoeba population was gated on by size and 10,000 amoeba events were collected for samples where amoebae were incubated alone or with red blood cells at a 1:10 ratio, a 1:100 ratio. 100,000 events were collected for amoebae incubated with red blood cells at a 1:1000 ratio. Data are from 6 replicates from 3 independent experiments. See Figure S3 for the analysis gating scheme.

For C3b experiments, amoebae were labeled with CMFDA and Jurkat cells were left unlabeled. Amoebae and Jurkats were incubated together at a 1:40 amoebae: Jurkat ratio. After fixation, samples were blocked in 1 x PBST containing 5% BSA and 20% Normal Goat Serum for 30 minutes at room temperature on a rocker. Samples were then labeled with a mouse monoclonal antibody to complement components C3b and iC3b (Clone E7; MilliporeSigma) diluted 1:100 in blocking solution at 4°C overnight on a rocker. Samples were washed in 1 x PBST and labeled with an Alexa Fluor 47 AffiniPure Fab Fragment Donkey Anti-Mouse secondary antibody (Jackson ImmunoResearch Laboratories, Inc) stored in 50% glycerol (Sigma-Aldrich). The secondary antibody was diluted 1:100 in blocking solution for a final dilution of 1:200, and samples were incubated for 3 hours at room temperature on a rocker. Samples were washed in 1 x PBST, resuspended in 50 µl 1 x PBS, and run on an Amnis ImageStreamX Mark II. 10,000 events were collected in samples were amoebae were incubated alone and 100,000 events were collected in samples where amoebae were incubated with Jurkat cells. Data are from 6 replicates across 3 independent experiments. See Figure S4 for the analysis gating scheme.

Statistical analysis

22 GraphPad Prism software was used to perform all statistical analyses and the means and standard

23 deviation values are displayed on all data plots. Analyses were done using a Student's unpaired t test (no

24 significant difference was indicated by a P of >0.05; *, $P \leq 0.05$; **, $P \leq 0.01$; ***, $P \leq 0.001$; ****, $P \leq 0.0001$).

ACKNOWLEDGMENTS

We thank Dr. Scott Dawson, Dr. Stephen McSorley, and the members of our laboratory for helpful discussions. All ImageStream and confocal data were acquired using shared instrumentation in the UC Davis MCB Light Microscopy Imaging Facility. We thank Dr. Michael Paddy for technical support in the use of these instruments. This work was funded by NIH grant AI146914 and a Pew Scholarship awarded to K.S.R.

AUTHOR CONTRIBUTIONS

H.W.M. designed and performed the experiments. T.S.Y.T. contributed intellectually to the studies and performed support experiments not included in the final paper. K.S.R. conceived of the overall approach and oversaw the design and analysis of the experiments. H.W.M. and K.S.R. wrote the manuscript.

REFERENCES

1. Wang H, Naghavi M, Allen C, Barber RM, Bhutta ZA, Carter A, Casey DC, Charlson FJ, Chen AZ, Coates MM, Coggeshall M, Dandona L, Dicker DJ, Erskine HE, Ferrari AJ, Fitzmaurice C, Foreman K, Forouzanfar MH, Fraser MS, Fullman N, Gething PW, Goldberg EM, Graetz N, Haagsma JA, Hay SI, Huynh C, Johnson CO, Kassebaum NJ, Kinfu Y, Kulikoff XR, Kutz M, Kyu HH, Larson HJ, Leung J, Liang X, Lim SS, Lind M, Lozano R, Marquez N, Mensah GA, Mikesell J, Mokdad AH, Mooney MD, Nguyen G, Nsoesie E, Pigott DM, Pinho C, Roth GA, Salomon JA, Sandar L, Silpakit N, Sligar A, Sorensen RJD, Stanaway J, Steiner C, Teeple S, Thomas BA, Troeger C, VanderZanden A, Vollset SE, Wanga V, Whiteford HA, Wolock T, Zoeckler L, Abate KH, Abbafati C, Abbas KM, Abd-Allah F, Abera SF, Abreu DMX, Abu-Raddad LJ, Abyu GY, Achoki T, Adelekan AL, Ademi Z, Adou AK, Adsuar JC, Afanvi KA, Afshin A, Agardh EE, Agarwal A, Agrawal A, Kiadaliri AA, Ajala ON, Akanda AS, Akinyemi RO, Akinyemiju TF, Akseer N, Lami FHA, Alabed S, Al-Aly Z, Alam K, Alam NKM, Alasfoor D, Aldhahri SF, Aldridge RW, Alegretti MA, Aleman AV, Alemu ZA, Alexander LT, Alhabib S, Ali R, Alkerwi A, Alla F, Allebeck P, Al-Raddadi R, Alsharif U, Altirkawi KA, Martin EA, Alvis-Guzman N, Amare AT, Amegah AK, Ameh EA, Amini H, Ammar W, Amrock SM, Andersen HH, Anderson BO, Anderson GM, Antonio CAT, Aregay AF, Ärnlöv J, Arsenijevic VSA, Artaman A, Asayesh H, Asghar RJ, Atique S, Avokpaho EFGA, Awasthi A, Azzopardi P, Bacha U, Badawi A, Bahit MC, Balakrishnan K, Banerjee A, Barac A, Barker-Collo SL, Bärnighausen T, Barregard L, Barrero LH, Basu A, Basu S, Bayou YT, Bazargan-Hejazi S, Beardsley J, Bedi N, Beghi E, Belay HA, Bell B, Bell ML, Bello AK, Bennett DA, Bensenor IM, Berhane A, Bernabé E, Betsu BD, Beyene AS, Bhala N, Bhalla A, Biadgilign S, Bikbov B, Abdulhak AAB, Biroscak BJ, Biryukov S, Bjertness E, Blore JD, Blosser CD, Bohensky MA, Borschmann R, Bose D, Bourne RRA, Brainin M, Brayne CEG, Brazinova A, Breitborde NJK, Brenner H, Brewer JD, Brown A, Brown J, Brugha TS, Buckle GC, Butt ZA, Calabria B, Campos-Nonato IR, Campuzano JC, Carapetis JR, Cárdenas R, Carpenter DO, Carrero JJ, Castañeda-Orjuela CA, Rivas JC, Catalá-López F, Cavalleri F, Cercy K, Cerda J, Chen W, Chew A, Chiang PP-C, Chibalabala M, Chibueze CE, Chimed-Ochir O, Chisumpa VH, Choi J-YJ, Chowdhury R, Christensen H,

58 Christopher DJ, Ciobanu LG, Cirillo M, Cohen AJ, Colistro V, Colomar M, Colquhoun SM, Cooper C, Cooper
59 LT, Cortinovis M, Cowie BC, Crump JA, Damsere-Derry J, Danawi H, Dandona R, Daoud F, Darby SC, Dargan
60 PI, das Neves J, Davey G, Davis AC, Davitoiu DV, de Castro EF, de Jager P, Leo DD, Degenhardt L, Dellavalle
61 RP, Deribe K, Deribew A, Dharmaratne SD, Dhillon PK, Diaz-Torné C, Ding EL, dos Santos KPB, Dossou E,
62 Driscoll TR, Duan L, Dubey M, Duncan BB, Ellenbogen RG, Ellingsen CL, Elyazar I, Endries AY, Ermakov SP,
63 Eshrati B, Esteghamati A, Estep K, Faghmous IDA, Fahimi S, Faraon EJA, Farid TA, Farinha CS e S, Faro A,
64 Farvid MS, Farzadfar F, Feigin VL, Fereshtehnejad S-M, Fernandes JG, Fernandes JC, Fischer F, Fitchett JRA,
65 Flaxman A, Foigt N, Fowkes FGR, Franca EB, Franklin RC, Friedman J, Frostad J, Fürst T, Futran ND, Gall SL,
66 Gambashidze K, Gamkrelidze A, Ganguly P, Gankpé FG, Gebre T, Gebrehiwot TT, Gebremedhin AT, Gebru
67 AA, Geleijnse JM, Gessner BD, Ghoshal AG, Gibney KB, Gillum RF, Gilmour S, Giref AZ, Giroud M, Gishu MD,
68 Giussani G, Glaser E, Godwin WW, Gomez-Dantes H, Gona P, Goodridge A, Gopalani SV, Gosselin RA,
69 Gotay CC, Goto A, Gouda HN, Greaves F, Gugnani HC, Gupta R, Gupta R, Gupta V, Gutiérrez RA, Hafezi-
70 Nejad N, Haile D, Hailu AD, Hailu GB, Halasa YA, Hamadeh RR, Hamidi S, Hancock J, Handal AJ, Hankey GJ,
71 Hao Y, Harb HL, Harikrishnan S, Haro JM, Havmoeller R, Heckbert SR, Heredia-Pi IB, Heydarpour P,
72 Hilderink HBM, Hoek HW, Hogg RS, Horino M, Horita N, Hosgood HD, Hotez PJ, Hoy DG, Hsairi M, Htet AS,
73 Htike MMT, Hu G, Huang C, Huang H, Huiart L, Husseini A, Huybrechts I, Huynh G, Iburg KM, Innos K, Inoue
74 M, Iyer VJ, Jacobs TA, Jacobsen KH, Jahanmehr N, Jakovljevic MB, James P, Javanbakht M, Jayaraman SP,
75 Jayatilleke AU, Jeemon P, Jensen PN, Jha V, Jiang G, Jiang Y, Jibat T, Jimenez-Corona A, Jonas JB, Joshi TK,
76 Kabir Z, Kamal R, Kan H, Kant S, Karch A, Karema CK, Karimkhani C, Karletsos D, Karthikeyan G, Kasaeian A,
77 Katibeh M, Kaul A, Kawakami N, Kayibanda JF, Keiyoro PN, Kemmer L, Kemp AH, Kengne AP, Keren A,
78 Kereselidze M, Kesavachandran CN, Khader YS, Khalil IA, Khan AR, Khan EA, Khang Y-H, Khera S, Khoja
79 TAM, Kieling C, Kim D, Kim YJ, Kissela BM, Kissoon N, Knibbs LD, Knudsen AK, Kokubo Y, Kolte D, Kopec JA,
80 Kosen S, Koul PA, Koyanagi A, Krog NH, Defo BK, Bicer BK, Kudom AA, Kuipers EJ, Kulkarni VS, Kumar GA,
81 Kwan GF, Lal A, Lal DK, Lalloo R, Lallukka T, Lam H, Lam JO, Langan SM, Lansingh VC, Larsson A, Laryea DO,

Latif AA, Lawrynowicz AEB, Leigh J, Levi M, Li Y, Lindsay MP, Lipshultz SE, Liu PY, Liu S, Liu Y, Lo L-T, Logroscino G, Lotufo PA, Lucas RM, Lunevicius R, Lyons RA, Ma S, Machado VMP, Mackay MT, MacLachlan JH, Razek HMAE, Magdy M, Razek AE, Majdan M, Majeed A, Malekzadeh R, Manamo WAA, Mandisarisa J, Mangalam S, Mapoma CC, Marcenes W, Margolis DJ, Martin GR, Martinez-Raga J, Marzan MB, Masiye F, Mason-Jones AJ, Massano J, Matzopoulos R, Mayosi BM, McGarvey ST, McGrath JJ, McKee M, McMahon BJ, Meaney PA, Mehari A, Mehndiratta MM, Mejia-Rodriguez F, Mekonnen AB, Melaku YA, Memiah P, Memish ZA, Mendoza W, Meretoja A, Meretoja TJ, Mhimbira FA, Micha R, Millear A, Miller TR, Mirarefin M, Misganaw A, Mock CN, Mohammad KA, Mohammadi A, Mohammed S, Mohan V, Mola GLD, Monasta L, Hernandez JCM, Montero P, Montico M, Montine TJ, Moradi-Lakeh M, Morawska L, Morgan K, Mori R, Mozaffarian D, Mueller UO, Murthy GVS, Murthy S, Musa KI, Nachega JB, Nagel G, Naidoo KS, Naik N, Naldi L, Nangia V, Nash D, Nejjari C, Neupane S, Newton CR, Newton JN, Ng M, Ngalesoni FN, de Dieu Ngirabega J, Nguyen QL, Nisar MI, Pete PMN, Nomura M, Norheim OF, Norman PE, Norrving B, Nyakarahuka L, Ogbo FA, Ohkubo T, Ojelabi FA, Olivares PR, Olusanya BO, Olusanya JO, Opio JN, Oren E, Ortiz A, Osman M, Ota E, Ozdemir R, Pa M, Pain A, Pandian JD, Pant PR, Papachristou C, Park E-K, Park J-H, Parry CD, Parsaeian M, Caicedo AJP, Patten SB, Patton GC, Paul VK, Pearce N, Pedro JM, Stokic LP, Pereira DM, Perico N, Pesudovs K, Petzold M, Phillips MR, Piel FB, Pillay JD, Plass D, Platts-Mills JA, Polinder S, Pope CA, Popova S, Poulton RG, Pourmalek F, Prabhakaran D, Qorbani M, Quame-Amaglo J, Quistberg DA, Rafay A, Rahimi K, Rahimi-Movaghar V, Rahman M, Rahman MHU, Rahman SU, Rai RK, Rajavi Z, Rajsic S, Raju M, Rakovac I, Rana SM, Ranabhat CL, Rangaswamy T, Rao P, Rao SR, Refaat AH, Rehm J, Reitsma MB, Remuzzi G, Resnikoff S, Ribeiro AL, Ricci S, Blancas MJR, Roberts B, Roca A, Rojas-Rueda D, Ronfani L, Roshandel G, Rothenbacher D, Roy A, Roy NK, Ruhago GM, Sagar R, Saha S, Sahathevan R, Saleh MM, Sanabria JR, Sanchez-Niño MD, Sanchez-Riera L, Santos IS, Sarmiento-Suarez R, Sartorius B, Satpathy M, Savic M, Sawhney M, Schaub MP, Schmidt MI, Schneider IJC, Schöttker B, Schutte AE, Schwebel DC, Seedat S, Sepanlou SG, Servan-Mori EE, Shackelford KA, Shaddick G, Shaheen A, Shahraz S, Shaikh MA, Shakh-Nazarova M, Sharma R, She J,

Sheikhbahaei S, Shen J, Shen Z, Shepard DS, Sheth KN, Shetty BP, Shi P, Shibuya K, Shin M-J, Shiri R, Shiue I, Shrime MG, Sigfusdottir ID, Silberberg DH, Silva DAS, Silveira DGA, Silverberg JI, Simard EP, Singh A, Singh GM, Singh JA, Singh OP, Singh PK, Singh V, Soneji S, Søreide K, Soriano JB, Sposato LA, Sreeramareddy CT, Stathopoulou V, Stein DJ, Stein MB, Stranges S, Stroumpoulis K, Sunguya BF, Sur P, Swaminathan S, Sykes BL, Szoeke CEI, Tabarés-Seisdedos R, Tabb KM, Takahashi K, Takala JS, Talongwa RT, Tandon N, Tavakkoli M, Taye B, Taylor HR, Ao BJT, Tedla BA, Tefera WM, Have MT, Terkawi AS, Tesfay FH, Tessema GA, Thomson AJ, Thorne-Lyman AL, Thrift AG, Thurston GD, Tillmann T, Tirschwell DL, Tonelli M, Topor-Madry R, Topouzis F, Towbin JA, Traebert J, Tran BX, Truelsen T, Trujillo U, Tura AK, Tuzcu EM, Uchendu US, Ukwaja KN, Undurraga EA, Uthman OA, Dingenen RV, van Donkelaar A, Vasankari T, Vasconcelos AMN, Venketasubramanian N, Vidavalur R, Vijayakumar L, Villalpando S, Violante FS, Vlassov VV, Wagner JA, Wagner GR, Wallin MT, Wang L, Watkins DA, Weichenthal S, Weiderpass E, Weintraub RG, Werdecker A, Westerman R, White RA, Wijeratne T, Wilkinson JD, Williams HC, Wiysonge CS, Woldeyohannes SM, Wolfe CDA, Won S, Wong JQ, Woolf AD, Xavier D, Xiao Q, Xu G, Yakob B, Yalew AZ, Yan LL, Yano Y, Yaseri M, Ye P, Yebyo HG, Yip P, Yirsaw BD, Yonemoto N, Yonga G, Younis MZ, Yu S, Zaidi Z, Zaki MES, Zannad F, Zavala DE, Zeeb H, Zeleke BM, Zhang H, Zodpey S, Zonies D, Zuhlke LJ, Vos T, Lopez AD, Murray CJL. 2016. Global, regional, and national life expectancy, all-cause mortality, and cause-specific mortality for 249 causes of death, 1980–2015: a systematic analysis for the Global Burden of Disease Study 2015. The Lancet 388:1459–1544.

2. Marie C, Petri WA. 2013. Amoebic dysentery. BMJ Clin Evid 2013:0918.

3. Alvarado-Esquivel C, Hernandez-Tinoco J, Sanchez-Anguiano LF. 2015. Seroepidemiology of Entamoeba histolytica Infection in General Population in Rural Durango, Mexico. J Clin Med Res 7:435–439.

4. Gilchrist CA, Petri SE, Schneider BN, Reichman DJ, Jiang N, Begum S, Watanabe K, Jansen CS, Elliott KP, Burgess SL, Ma JZ, Alam M, Kabir M, Haque R, Petri WA. 2016. Role of the Gut Microbiota of Children in Diarrhea Due to the Protozoan Parasite Entamoeba histolytica. J Infect Dis 213:1579–1585.

5. Haque R, Huston CD, Hughes M, Houpt E, Petri WA. 2003. Amebiasis. New England Journal of Medicine 348:1565–1573.

6. Petri WA, Haque R, Mann BJ. 2002. The Bittersweet Interface of Parasite and Host: Lectin-Carbohydrate Interactions During Human Invasion by the Parasite Entamoeba histolytica. Annu Rev Microbiol 56:39–64.

7. Reed SL, Curd JG, Gigli I, Gillin FD, Braude AI. 1986. Activation of complement by pathogenic and nonpathogenic Entamoeba histolytica. J Immunol 136:2265–2270.

8. Costa CA, Nunes ÁC, Ferreira AJ, Gomes MA, Caliari MV. 2010. Entamoeba histolytica and E. dispar trophozoites in the liver of hamsters: in vivo binding of antibodies and complement. Parasites & Vectors 3:23.

9. Reed SL, Ember JA, Herdman DS, DiScipio RG, Hugli TE, Gigli I. 1995. The extracellular neutral cysteine proteinase of Entamoeba histolytica degrades anaphylatoxins C3a and C5a. J Immunol 155:266–274.

10. Reed SL, Gigli I. 1990. Lysis of complement-sensitive Entamoeba histolytica by activated terminal complement components. Initiation of complement activation by an extracellular neutral cysteine proteinase. J Clin Invest 86:1815–1822.

11. Reed SL, Keene WE, McKerrow JH, Gigli I. 1989. Cleavage of C3 by a neutral cysteine proteinase of Entamoeba histolytica. J Immunol 143:189–195.

12. Braga LL, Ninomiya H, McCoy JJ, Eacker S, Wiedmer T, Pham C, Wood S, Sims PJ, Petri WA. 1992. Inhibition of the complement membrane attack complex by the galactose-specific adhesion of Entamoeba histolytica. J Clin Invest 90:1131–1137.

13. Miller HW, Suleiman RL, Ralston KS. 2019. Trogocytosis by Entamoeba histolytica Mediates Acquisition and Display of Human Cell Membrane Proteins and Evasion of Lysis by Human Serum. mBio 10:e00068-19.

14. Bettadapur A, Miller HW, Ralston KS. 2020. Biting Off What Can Be Chewed: Trogocytosis in Health, Infection, and Disease. Infect Immun 88:e00930-19.

15. Ralston KS, Solga MD, Mackey-Lawrence NM, Somlata null, Bhattacharya A, Petri WA. 2014. Trogocytosis by Entamoeba histolytica contributes to cell killing and tissue invasion. Nature 508:526–530.

16. González-Ruiz A, Haque R, Aguirre A, Castañón G, Hall A, Guhl F, Ruiz-Palacios G, Miles MA, Warhurst DC. 1994. Value of microscopy in the diagnosis of dysentery associated with invasive Entamoeba histolytica. J Clin Pathol 47:236–239.

17. Davies A, Simmons DL, Hale G, Harrison RA, Tighe H, Lachmann PJ, Waldmann H. 1989. CD59, an LY-6-like protein expressed in human lymphoid cells, regulates the action of the complement membrane attack complex on homologous cells. Journal of Experimental Medicine 170:637–654.

18. Štefanová I, Hilgert I, Krištofová H, Brown R, Low MG, Hořejši V. 1989. Characterization of a broadly expressed human leucocyte surface antigen MEM-43 anchored in membrane through phosphatidylinositol. Molecular Immunology 26:153–161.

19. Cinek T, Horejsí V. 1992. The nature of large noncovalent complexes containing glycosyl-phosphatidylinositol-anchored membrane glycoproteins and protein tyrosine kinases. The Journal of Immunology 149:2262–2270.

20. Rollins SA, Sims PJ. 1990. The complement-inhibitory activity of CD59 resides in its capacity to block incorporation of C9 into membrane C5b-9. J Immunol 144:3478–3483.

21. Meri S, Morgan BP, Davies A, Daniels RH, Olavesen MG, Waldmann H, Lachmann PJ. 1990. Human protectin (CD59), an 18,000-20,000 MW complement lysis restricting factor, inhibits C5b-8 catalysed insertion of C9 into lipid bilayers. Immunology 71:1–9.

22. Zhao J, Rollins SA, Maher SE, Bothwell AL, Sims PJ. 1991. Amplified gene expression in CD59-transfected Chinese hamster ovary cells confers protection against the membrane attack complex of human complement. J Biol Chem 266:13418–13422.

23. Ventura-Juárez J, Campos-Rodríguez R, Jarillo-Luna RA, Muñoz-Fernández L, Escario-G-Trevijano JA, Pérez-Serrano J, Quintanar JL, Salinas E, Villalobos-Gómez FR. 2009. Trophozoites of Entamoeba histolytica express a CD59-like molecule in human colon. Parasitol Res 104:821–826.

24. Goslings WR, Blom DJ, de Waard-Siebinga I, van Beelen E, Claas FH, Jager MJ, Gorter A. 1996. Membrane-bound regulators of complement activation in uveal melanomas. CD46, CD55, and CD59 in uveal melanomas. Invest Ophthalmol Vis Sci 37:1884–1891.

25. Varsano S, Rashkovsky L, Shapiro H, Ophir D, Mark-Bentankur T. 1998. Human lung cancer cell lines express cell membrane complement inhibitory proteins and are extremely resistant to complement-mediated lysis; a comparison with normal human respiratory epithelium in vitro, and an insight into mechanism(s) of resistance. Clin Exp Immunol 113:173–182.

26. Nicholson-Weller A, Burge J, Fearon DT, Weller PF, Austen KF. 1982. Isolation of a human erythrocyte membrane glycoprotein with decay-accelerating activity for C3 convertases of the complement system. The Journal of Immunology 129:184–189.

38 27. Medof ME, Kinoshita T, Nussenzweig V. 1984. Inhibition of complement activation on the surface of cells
39 after incorporation of decay-accelerating factor (DAF) into their membranes. J Exp Med 160:1558–1578.

90 28. Wang G, Liszewski MK, Chan AC, Atkinson JP. 2000. Membrane Cofactor Protein (MCP; CD46): Isoform-
91 Specific Tyrosine Phosphorylation. The Journal of Immunology 164:1839–1846.

92 29. Riley-Vargas RC, Gill DB, Kemper C, Liszewski MK, Atkinson JP. 2004. CD46: expanding beyond complement
93 regulation. Trends in Immunology 25:496–503.

94 30. Liszewski MK, Atkinson JP. 2015. Complement regulator CD46: genetic variants and disease associations.
95 Human Genomics 9:7.

96 31. Seya T, Turner JR, Atkinson JP. 1986. Purification and characterization of a membrane protein (gp45-70)
97 that is a cofactor for cleavage of C3b and C4b. J Exp Med 163:837–855.

98 32. Fishelson Z, Donin N, Zell S, Schultz S, Kirschfink M. 2003. Obstacles to cancer immunotherapy: expression
99 of membrane complement regulatory proteins (mCRPs) in tumors. Molecular Immunology 40:109–123.

00 33. Gelderman KA, Blok VT, Fleuren GJ, Gorter A. 2002. The Inhibitory Effect of CD46, CD55, and CD59 on
01 Complement Activation After Immunotherapeutic Treatment of Cervical Carcinoma Cells with Monoclonal
02 Antibodies or Bispecific Monoclonal Antibodies. Lab Invest 82:483–493.

03 34. Jurianz K, Maslak S, Garcia-Schüler H, Fishelson Z, Kirschfink M. 1999. Neutralization of complement
04 regulatory proteins augments lysis of breast carcinoma cells targeted with rhumAb anti-HER2.
05 Immunopharmacology 42:209–218.

06 35. Cong L, Ran FA, Cox D, Lin S, Barretto R, Habib N, Hsu PD, Wu X, Jiang W, Marraffini LA, Zhang F. 2013.
07 Multiplex genome engineering using CRISPR/Cas systems. Science 339:819–823.

36. Thielen AJF, van Baarsen IM, Jongsma ML, Zeerleder S, Spaapen RM, Wouters D. 2018. CRISPR/Cas9 generated human CD46, CD55 and CD59 knockout cell lines as a tool for complement research. Journal of Immunological Methods 456:15–22.

37. Schindelin J, Arganda-Carreras I, Frise E, Kaynig V, Longair M, Pietzsch T, Preibisch S, Rueden C, Saalfeld S, Schmid B, Tinevez J-Y, White DJ, Hartenstein V, Eliceiri K, Tomancak P, Cardona A. 2012. Fiji: an open-source platform for biological-image analysis. Nat Methods 9:676–682.

FIGURE LEGENDS

Fig 1: Amoebic protection from complement following trogocytosis is dose-dependent.

Amoebae were labeled with CMFDA cytoplasm dye and incubated alone or with increasing concentrations of human Jurkat cells or primary human red blood cells. Human cells were labeled with DiD membrane dye. Following exposure to human serum, amoeba death was assessed with Zombie Violet viability dye and ingested human cell material was determined by quantifying mean fluorescence intensity (MFI) of DiD present on amoebae. **(A)** Normalized MFI of DiD on amoebae incubated alone or with increasing concentrations of Jurkat cells. **(B)** Normalized death of amoebae from conditions in panel A. **(C)** Death of amoebae from conditions in panel A, expressed as percent protection. Percent protection was calculated by subtracting the total death of amoebae incubated with human cells from the total death of amoebae incubated alone. **(D)** Normalized MFI of DiD on amoebae incubated alone or with increasing concentrations of red blood cells. **(E)** Normalized death of amoebae from conditions in panel D. **(F)** Death of amoebae from conditions in panel D, expressed as percent protection. **(G)** Representative images of amoebae incubated with increasing concentrations of Jurkat cells. Amoebae are shown in green and ingested human cell material is shown in red. Data were analyzed by imaging flow cytometry and are from 6 replicates across 3 independent experiments. **(H)** Representative images of amoebae incubated with red blood cells. Data were analyzed by imaging flow cytometry and are from 6 replicates across 3 independent experiments.

Fig 2: Amoebic trogocytosis of human cells inhibits deposition of complement C3b.

Amoebae were incubated alone or in the presence of human Jurkat T cells and subsequently exposed to human serum. Viability was assessed with Zombie Violet dye. The presence of C3b was detected using a mouse monoclonal antibody to C3b and iC3b. **(A)** Death of amoebae that were incubated alone (open bar) or in the presence of human Jurkat T cells (filled bar). **(B)** Mean fluorescence intensity of deposited C3b on amoebae. **(C)** Deposited C3b on dead (open bar) or live (filled bar) amoebae. **(D)** Deposited C3b on dead or live amoebae that had been incubated alone (open circles) or in the presence of human Jurkat T cells (closed

39 circles). **(E)** Representative images of C3b deposition (red) on live or dead amoebae. Data were analyzed by
40 imaging flow cytometry and are from 6 replicates across 3 independent experiments.

41 **Fig 3: Amoebae acquire and display the complement regulatory protein CD59 from human cells.**
42 Amoebae were allowed to perform trogocytosis on human Jurkat T cells for 5 minutes or 1 hour, or were
43 incubated alone. Human CD59 (red) was detected on the amoebae surface by monoclonal antibody staining.
44 Amoebae were labeled with CMFDA (green) and human cell nuclei were labeled with Hoechst (blue). **(A)**
45 Representative images from amoebae incubated alone or amoebae that performed trogocytosis on human
46 Jurkat T cells for 5 minutes or 1 hour. Arrows indicate patches of displayed CD59 on the amoeba surface. **(B)**
47 3D rendering of Z stack images taken from amoebae that were incubated with human Jurkat T cells for 1 hour.
48 **(C)** Zoomed in image of amoebae that were incubated with human Jurkat T cells for 1 hour. Data were
49 analyzed by confocal microscopy. 136 Images were collected from 1 independent experiment.

50 **Fig. 4: The amount of displayed CD59 increases with increased trogocytosis of human cells.**
51 Acquired CD59 molecules were quantified on amoebae that were allowed to perform trogocytosis on human
52 Jurkat T cells for 5 minutes or 1 hour, or were incubated alone. **(A)** Masking strategy for analysis of displayed
53 CD59 on the amoeba surface. A mask was created in order to allow for the detection of CD59 that overlapped
54 with amoebae, while excluding CD59 on intact human cells attached to amoebae. The mask is displayed in
55 turquoise, as an overlay on the individual images. Amoebae were labeled with CMFDA (green), human cell
56 nuclei were labeled with Hoechst (blue), and CD59 was detected with a monoclonal antibody (red).
57 Extracellular human cell nuclei fluorescence was removed from the masked analysis area. The excluded area
58 around human cell nuclei was then dilated by 4 pixels to include the entire diameter of the intact extra-cellular
59 human cells and associated CD59. CD59 was analyzed in the remaining masked analysis area of each image to
60 allow for analysis of displayed patches of acquired CD59 on amoebae. **(B)** The normalized mean fluorescence
61 intensity of CD59 on amoebae after 5 minutes or 1 hour of trogocytosis or amoebae that were incubated
62 alone. To normalize the data, samples were normalized to the 1 hour of trogocytosis condition. **(C)**

Representative images of amoebae that had performed trogocytosis on human Jurkat T cells for 5 minutes or 1 hour. Arrows indicate displayed CD59. Data were analyzed by imaging flow cytometry and are from 5 replicates across 3 independent experiments. The no primary control condition was performed in 2 of 3 independent experiments and data are from 3 replicates.

Fig. 5: Removal of CD59 and CD46 is not sufficient to sensitize amoebae to complement lysis.

(A-D) Human Jurkat T cells deficient in CD59 or CD46 were constructed using CRISPR/Cas9. Immunofluorescence and imaging flow cytometry were used to quantify CD59 or CD46. **(A)** Representative images of CD59 antibody staining (red) in vector control human cells or CD59 mutants. **(B)** Intensity of CD59 antibody staining in vector control human cells (gray) or CD59 mutants (black). 99.5% of CD59 mutants were in the CD59-negative gate ("-CD59"), while 0.75% of vector control cells were in this gate. **(C)** Representative images of CD46 antibody staining (red) in vector control human cells or CD46 mutants. **(D)** Intensity of CD46 antibody staining in vector control human cells (gray) or CD46 mutants (black). 99.5% of CD46 mutants were in the CD46-negative gate ("-CD46"), while 0.27% of vector control cells were in this gate. **(E-F)** Amoebae were labeled with CMFDA cytoplasm dye and incubated alone or with human Jurkat T cells. Human cell lines were either vector control cells (VC), CD59 mutants (-CD59), or CD46 mutants (-CD46). Human cells were labeled with DiD membrane dye. Following exposure to human serum, amoeba death was assessed with Zombie Violet viability dye and ingested human cell material was determined by quantifying mean fluorescence intensity (MFI) of DiD present on amoebae. **(E)** Normalized death of amoebae. **(F)** Normalized mean fluorescence intensity of DiD on amoebae. Data were analyzed by imaging flow cytometry and are from 6 replicates across 3 independent experiments.

33 **TABLES**

34 **Table 1: Primers used in these studies.**

Purpose	Primer Name	F/R	Sequence
Cloning of guide RNAs into the pX330-U6-Chimeric_BB-CBh-hSpCas9 plasmid backbone	CD59 gRNA **(BbsI overhang)** CD59 gRNA **(BbsI overhang)** CD46 gRNA **(BbsI overhang)** CD46 gRNA **(BbsI overhang)**	Forward Reverse Forward Reverse	**CACC**GCAAGGAGGGTCTGTCCTGTT **AAAC**AACAGGACAGACCCTCCTTGC **CACC**GAAAGGGACACTCGCGGCGGC **AAAC**GCCGCCGCGAGTGTCCCTTTC
Sanger sequencing of CRISPR gRNA plasmids	GENEWIZ Universal Primer "U6"	Forward	GACTATCATATGCTTACCGT
BLAST-identified primer sets for specific PCR amplification of CD59 and CD46	CD59 PCR amplification CD59 PCR amplification CD46 PCR amplification CD46 PCR amplification	Forward Reverse Forward Reverse	TTGACTCACTGACCCTGATGG TATCCATTGGTGTCCCCAAGC ACAAATATGACGGCGAGCCA GGCTCAATCCCGAAAACACG
Sanger Sequencing of PCR product from CRIPSR knockout clones	CD59 sequencing CD46 sequencing	Forward Forward	GGGGCTTATAGGGACTGAGC ACCTCTCGAAGGCCAAGG

35

SUPPLEMENTAL MATERIAL

SUPPLEMENTAL FIGURE LEGENDS

Fig. S1: Removal of GPI-anchored surface proteins using phosphatidylinositol-specific phospholipase C.

Amoebae were labeled with CMFDA cytoplasm dye and incubated alone or with human Jurkat T cells. Human cells were labeled with DiD membrane dye. Samples were then treated with phosphatidylinositol-specific phospholipase C (PI-PLC) to remove GPI-anchored proteins, or heat-inactivated phosphatidylinositol-specific phospholipase C (HI-PI-PLC) as a control. Following exposure to human serum, amoeba death was assessed with Zombie Violet viability dye and ingested human cell material was determined by quantifying mean fluorescence intensity (MFI) of DiD present on amoebae. **(A)** Normalized death of amoebae. **(B)** Normalized mean fluorescence intensity of DiD on amoebae. Data were analyzed by imaging flow cytometry and are from 8 replicates across 4 independent experiments. The untreated control condition was performed 3 of 4 independent experiments and data are from 6 replicates.

Fig. S2: Sequencing analysis of Jurkat CRISPR/Cas9 mutants.

Chromatograms from Sanger sequencing analysis of Jurkat T cell CRISPR/Cas9 mutants. Chromatograms from CD59 mutants **(A)** and CD46 mutants **(B)** show that the gene sequence of the mutants is different from the vector control cells downstream of the gRNA/PAM sites.

Fig. S3: Gating strategy used for analysis of experiments with increasing numbers of human cells.

(A) Gating strategy for experiments with increasing numbers of Jurkat cells. Focused cells were gated on from total collected events, using Gradient RMS Bright Field. Single amoebae were gated using area and aspect ratio of CMFDA cytoplasm dye fluorescence. Dead amoebae were gated on using fluorescence intensity of Zombie Violet dye and side scatter. **(B)** Gating strategy for experiments with increasing numbers of red blood cells. Only amoeba events were collected for analysis and were gated on using bright field area and aspect ratio during data acquisition. Focused cells were gated on from total collected events, using Gradient RMS

Bright Field. Single amoebae were gated using area and aspect ratio of CMFDA cytoplasm dye fluorescence. Dead amoebae were gated on using fluorescence intensity of Zombie Violet dye and side scatter.

Fig. S4: Gating strategy used for analysis of C3b deposition experiments.

(A) Focused cells were gated on from total collected events, using Gradient RMS Bright Field. Single amoebae were gated using area and aspect ratio of CMFDA cytoplasm dye fluorescence. Dead amoebae were gated on using fluorescence intensity of Zombie Violet dye and side scatter. **(B)** Representative histograms of C3b fluorescence intensity of all single amoeba, live amoeba, or dead amoeba populations.

Fig. S5: Gating strategy used for analysis of CD59 displayed on amoebae after 5 minutes and 1 hour of trogocytosis.

A masking strategy was developed to quantify only fluorescence of CD59 present on the amoebae, and not on extracellular human cells. **(A)** Focused cells were gated on from total collected events, using Gradient RMS Bright Field. Single amoebae were gated using area and aspect ratio of CMFDA cytoplasm dye fluorescence. Next, fluorescence intensity of CD59 inside of the masked area was measured. **(B)** Representative images of bright field, amoeba cytoplasm, human cell nuclei, and CD59 fluorescence with the masked area (turquoise) applied as an overlay.

Fig. S6: Gating strategy used for analysis of experiments with CRISPR knockout mutants and PI-PLC treatment.

Only cell events were collected for analysis (to minimize collection of debris) and were gated on using bright field area and aspect ratio during data acquisition. Focused cells were gated on from total collected events, using Gradient RMS Bright Field. Single amoebae were gated using area and aspect ratio of CMFDA cytoplasm dye fluorescence. Amoebae were gated on a second time using CMFDA fluorescence intensity and side scatter to eliminate remaining clumps of human cells from the analysis. Finally, dead amoebae were gated on using fluorescence intensity of Zombie Violet dye and side scatter.

Fig. 1

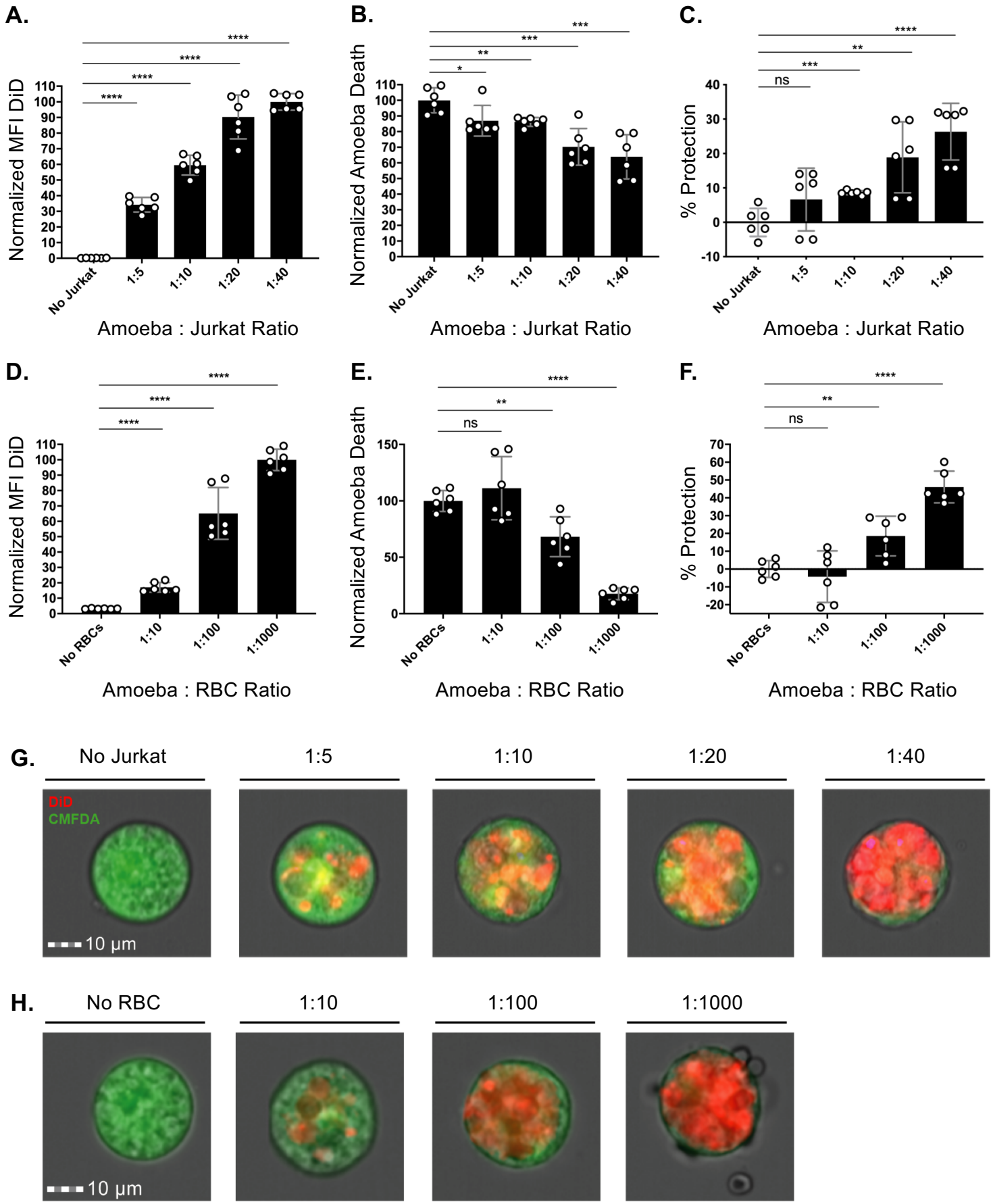
A.
Normalized MFI DiD
No Jurkat
1:5
1:10
1:20
1:40
Amoeba : Jurkat Ratio
B.
Normalized Amoeba Death
Amoeba : Jurkat Ratio
C.
% Protection
ns
Amoeba : Jurkat Ratio
D.
Normalized MFI DiD
No RBCs
1:10
1:100
1:1000
Amoeba : RBC Ratio
E.
Normalized Amoeba Death
ns
Amoeba : RBC Ratio
F.
% Protection
ns
Amoeba : RBC Ratio
G.
No Jurkat
1:5
1:10
1:20
1:40
DiD
CMFDA
10 µm
H.
No RBC
1:10
1:100
1:1000
10 µm

Fig. 2

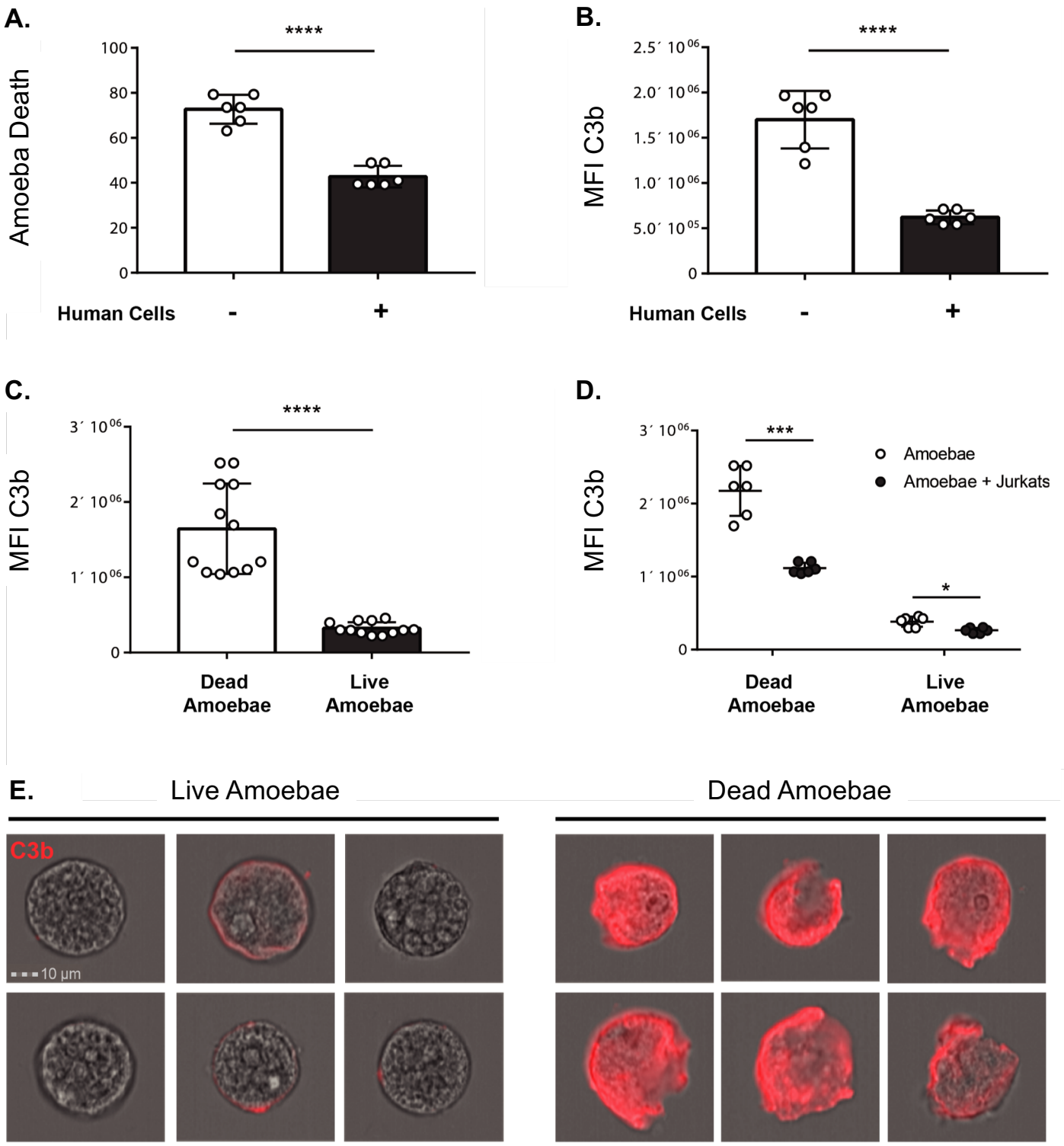
A.
Amoeba Death
100
80
60
40
20
0
****
Human Cells
-
+
B.
MFI C3b
2.5´ 10^06
2.0´ 10^06
1.5´ 10^06
1.0´ 10^06
5.0´ 10^05
0
****
Human Cells
-
+
C.
MFI C3b
3´ 10^06
2´ 10^06
1´ 10^06
0
****
Dead Amoebae
Live Amoebae
D.
MFI C3b
3´ 10^06
2´ 10^06
1´ 10^06
0
***
*
Amoebae
Amoebae + Jurkats
Dead Amoebae
Live Amoebae
E.
Live Amoebae
Dead Amoebae
C3b
10 µm

Fig. 3

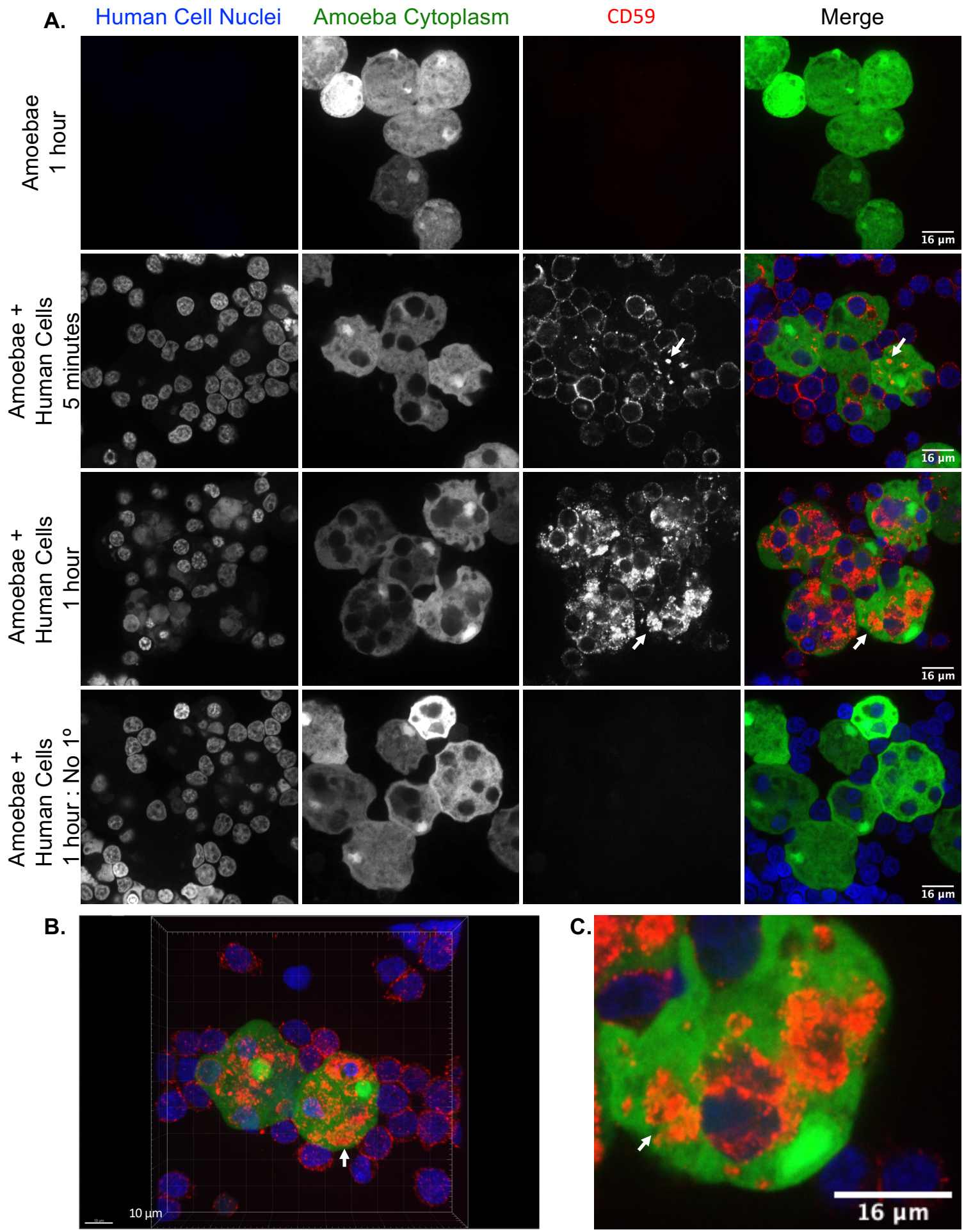
A.
Human Cell Nuclei
Amoeba Cytoplasm
CD59
Merge
Amoebae 1 hour
Amoebae + Human Cells 5 minutes
Amoebae + Human Cells 1 hour
Amoebae + Human Cells 1 hour : No 1°
16 µm
B.
10 µm
C.
16 µm

Fig. 4

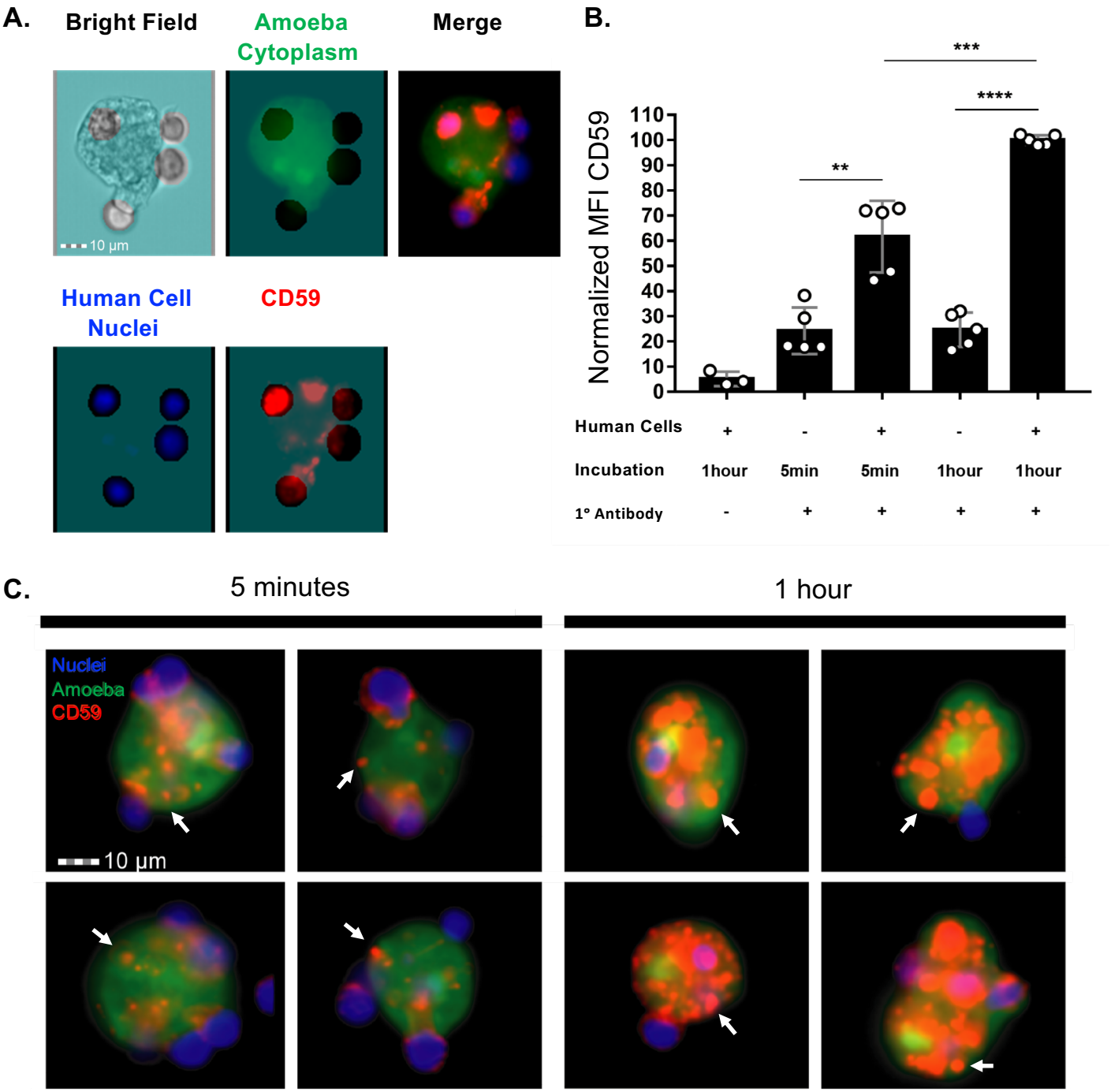
A.
Bright Field
Amoeba Cytoplasm
Merge
10 µm
Human Cell Nuclei
CD59
B.
Normalized MFI CD59
110
100
90
80
70
60
50
40
30
20
10
0
**
***
****
Human Cells + - + - +
Incubation 1hour 5min 5min 1hour 1hour
1° Antibody - + + + +
C.
5 minutes
1 hour
Nuclei
Amoeba
CD59
10 µm

Fig. 5

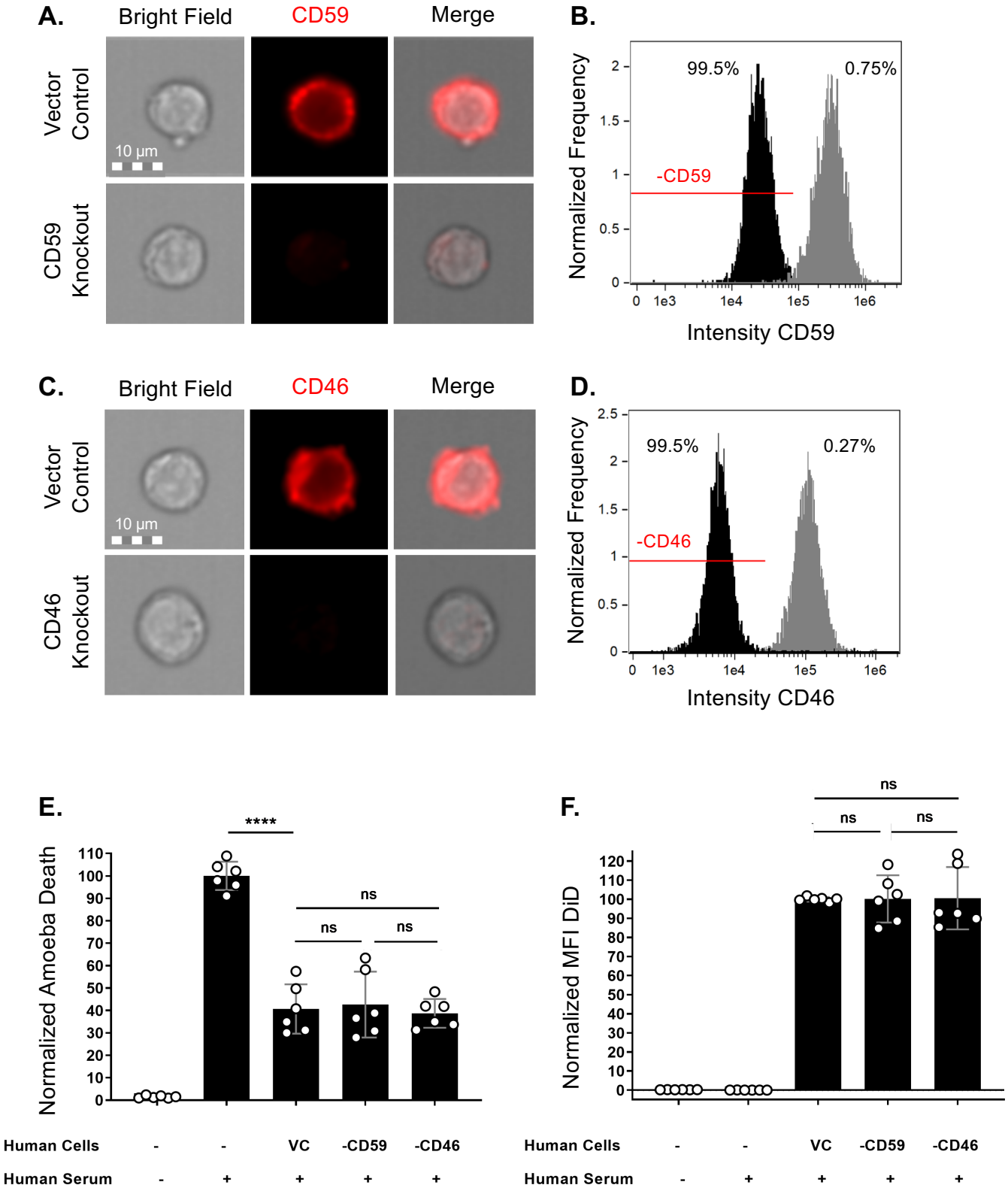
A.
Bright Field
CD59
Merge
Vector Control
CD59 Knockout
10 µm
B.
Normalized Frequency
99.5%
0.75%
-CD59
Intensity CD59
C.
Bright Field
CD46
Merge
Vector Control
CD46 Knockout
10 µm
D.
Normalized Frequency
99.5%
0.27%
-CD46
Intensity CD46
E.
Normalized Amoeba Death
****
ns
ns
ns
Human Cells - - VC -CD59 -CD46
Human Serum - + + + +
F.
Normalized MFI DiD
ns
ns
ns
Human Cells - - VC -CD59 -CD46
Human Serum - + + + +

Fig. S1

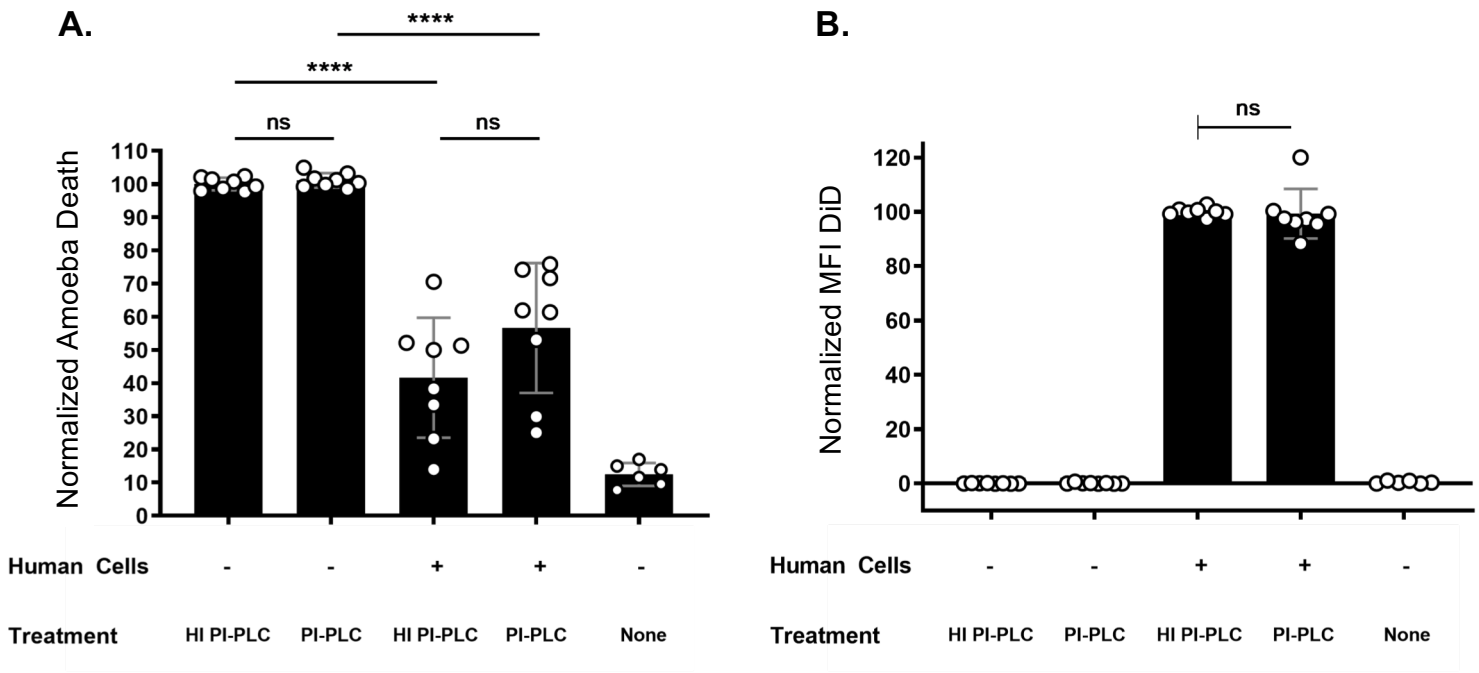
A.
****
****
ns
ns
Normalized Amoeba Death
110
100
90
80
70
60
50
40
30
20
10
0
Human Cells
-
-
+
+
-
Treatment
HI PI-PLC
PI-PLC
HI PI-PLC
PI-PLC
None
B.
ns
Normalized MFI DiD
120
100
80
60
40
20
0
Human Cells
-
-
+
+
-
Treatment
HI PI-PLC
PI-PLC
HI PI-PLC
PI-PLC
None

Fig. S2

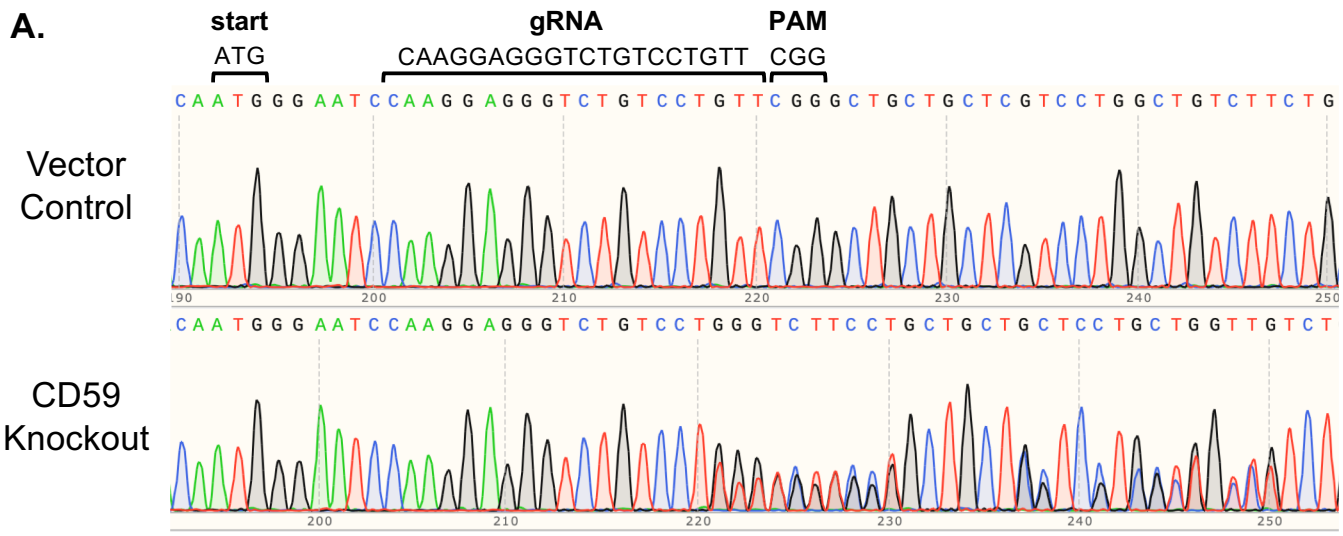
A.
start
ATG
gRNA
CAAGGAGGGTCTGTCCTGTT
PAM
CGG
Vector Control
CD59 Knockout

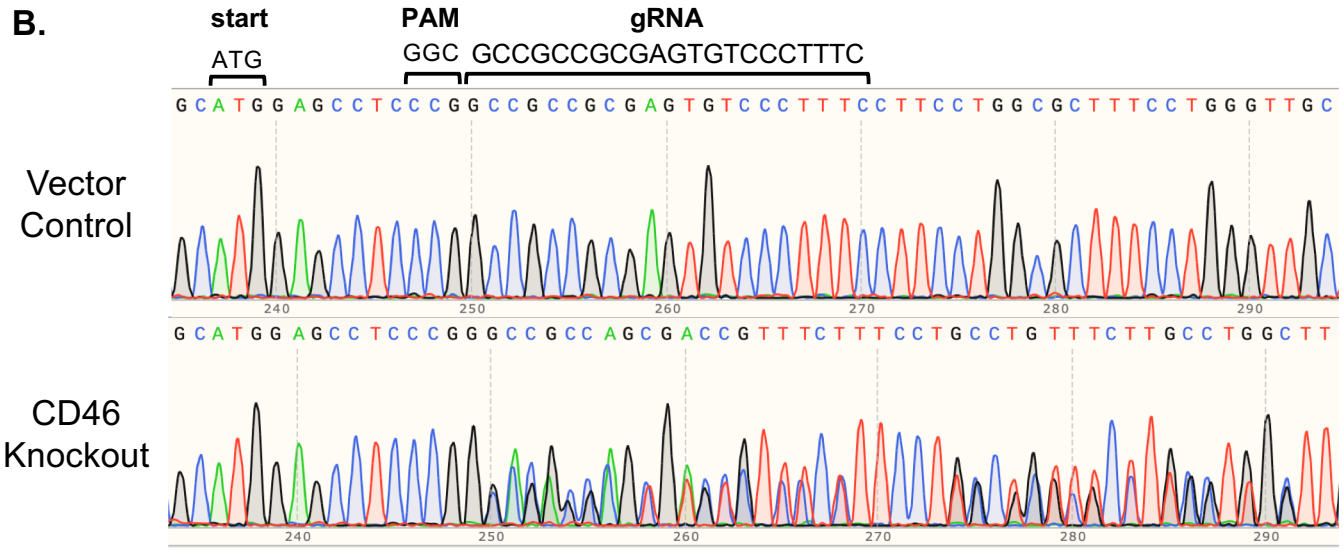
B.
start
ATG
PAM
GGC
gRNA
GCCGCCGCGAGTGTCCCTTTC
Vector Control
CD46 Knockout

Fig. S3

A.

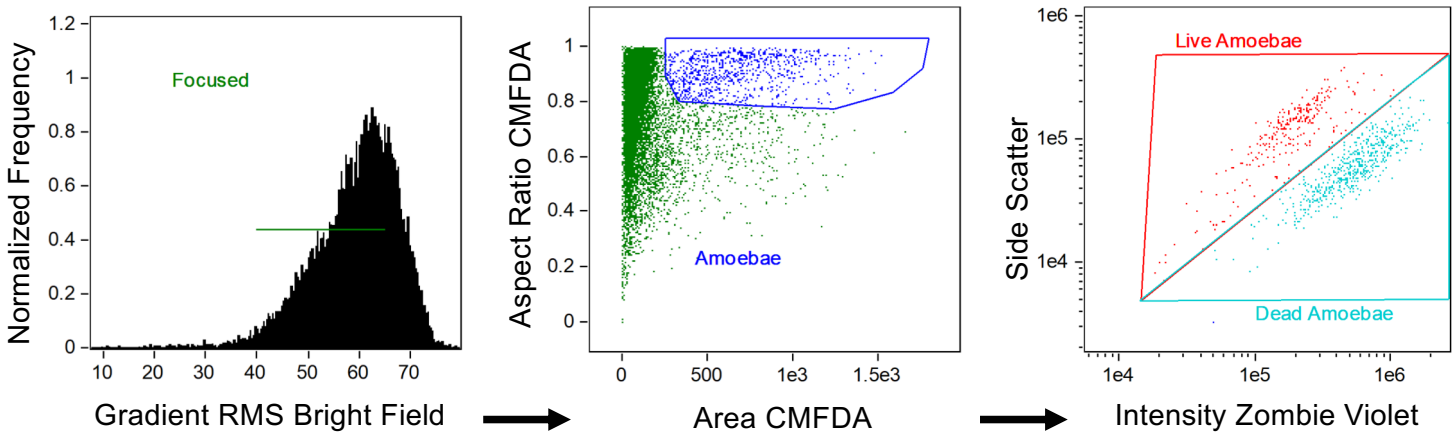
Normalized Frequency
Focused
Gradient RMS Bright Field
Aspect Ratio CMFDA
Amoebae
Area CMFDA
Side Scatter
Live Amoebae
Dead Amoebae
Intensity Zombie Violet

B.

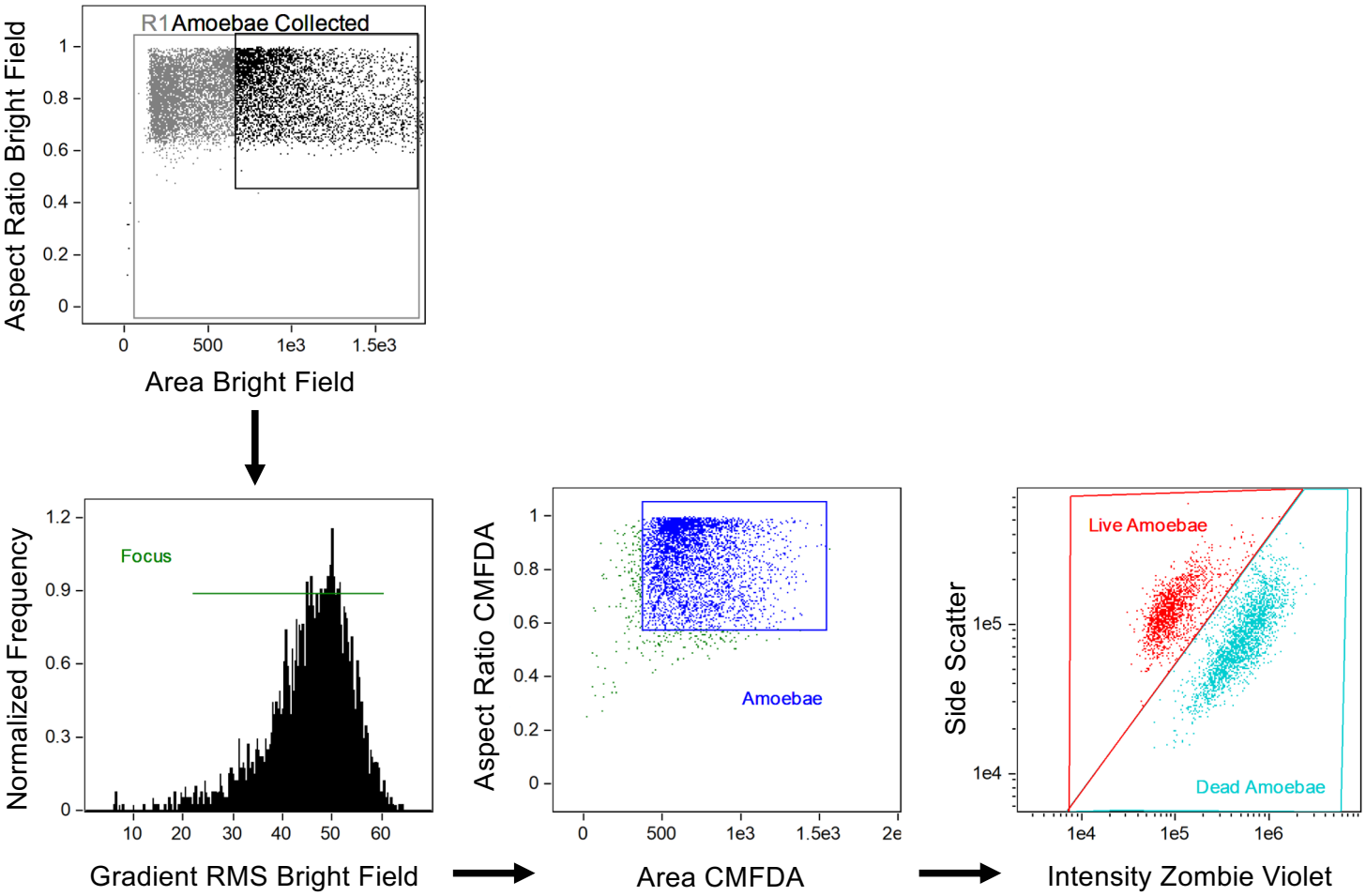
Aspect Ratio Bright Field
R1 Amoebae Collected
Area Bright Field
Normalized Frequency
Focus
Gradient RMS Bright Field
Aspect Ratio CMFDA
Amoebae
Area CMFDA
Side Scatter
Live Amoebae
Dead Amoebae
Intensity Zombie Violet

Fig. S4

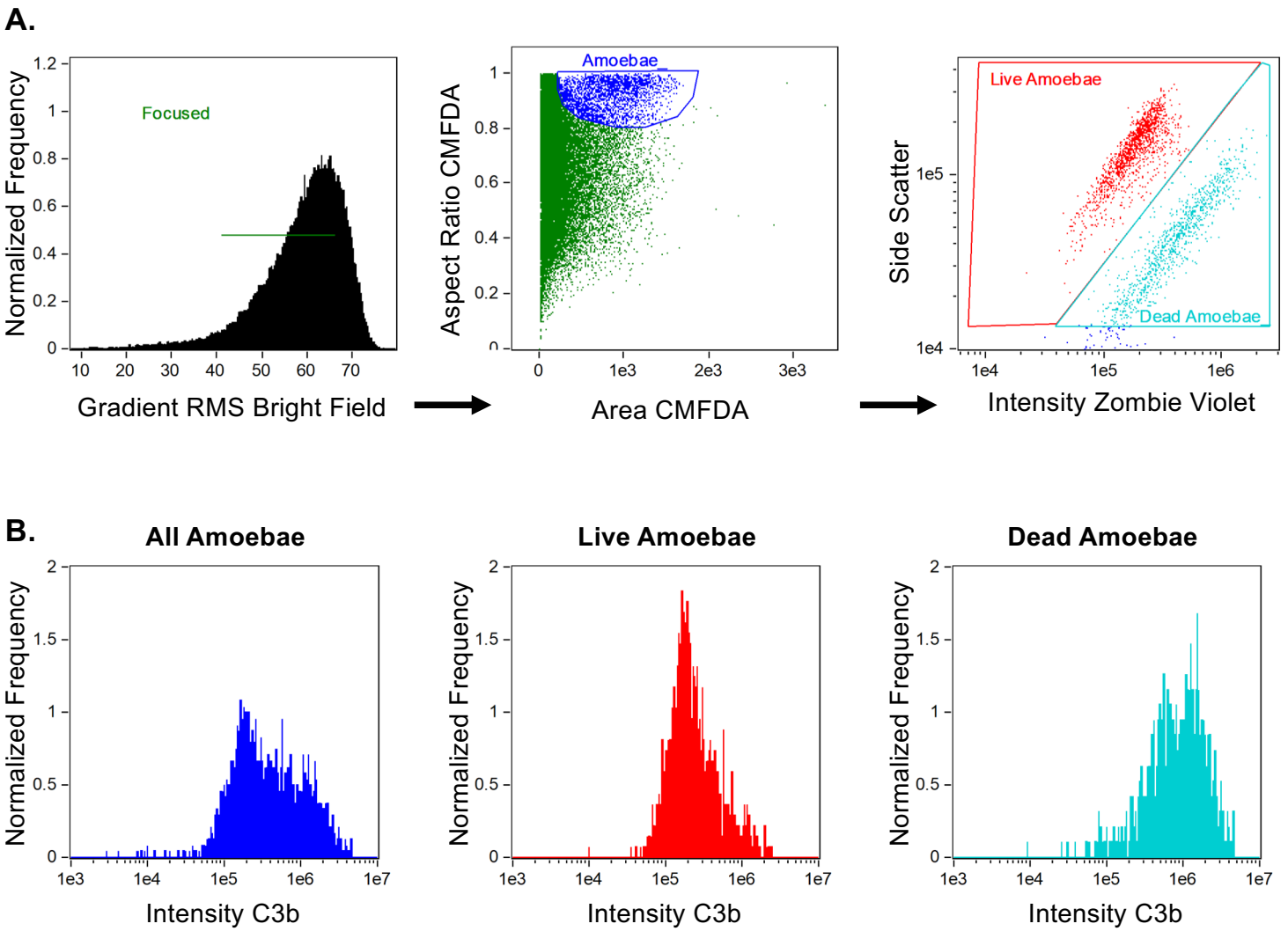
A.
Normalized Frequency
Focused
Gradient RMS Bright Field
Aspect Ratio CMFDA
Amoebae
Area CMFDA
Side Scatter
Live Amoebae
Dead Amoebae
Intensity Zombie Violet
B.
All Amoebae
Live Amoebae
Dead Amoebae
Normalized Frequency
Intensity C3b

Fig. S5

A.

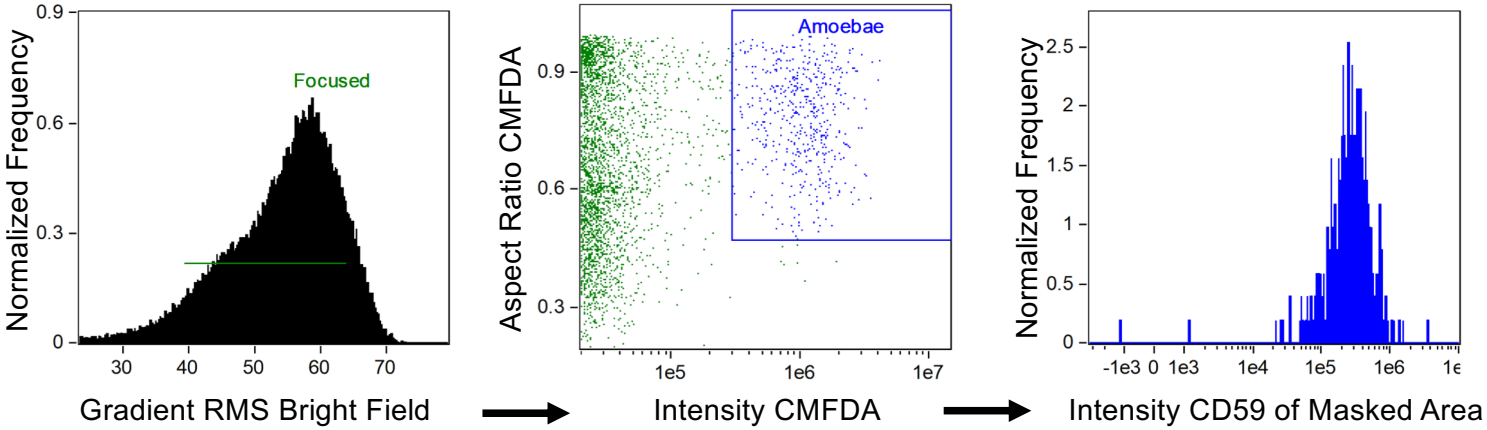
Normalized Frequency
0.9
0.6
0.3
0
Focused
30
40
50
60
70
Gradient RMS Bright Field
Aspect Ratio CMFDA
0.9
0.6
0.3
Amoebae
1e5
1e6
1e7
Intensity CMFDA
Normalized Frequency
2.5
2
1.5
1
0.5
0
-1e3 0 1e3
1e4
1e5
1e6
Intensity CD59 of Masked Area

B.

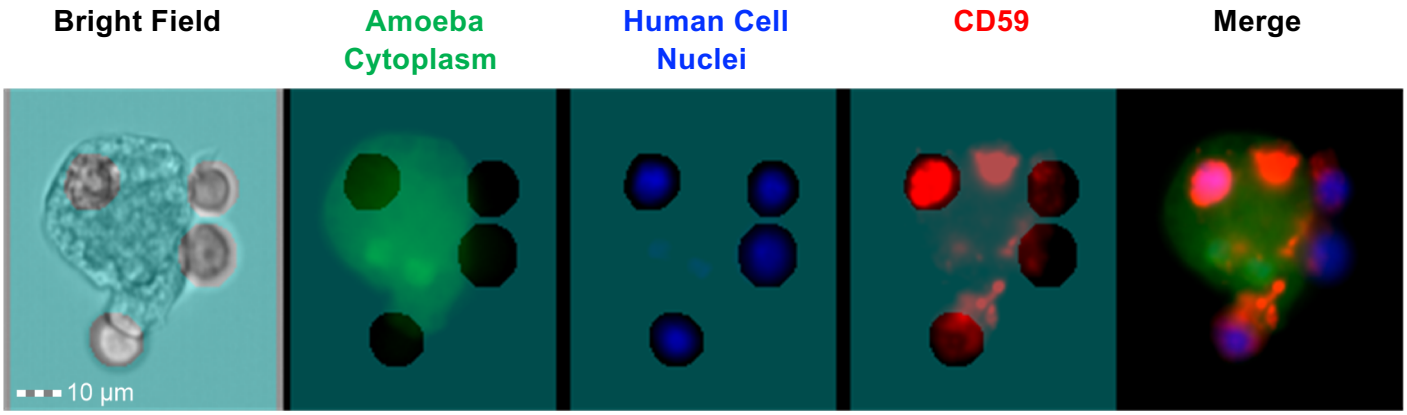
Bright Field
Amoeba Cytoplasm
Human Cell Nuclei
CD59
Merge
10 µm

Fig. S6

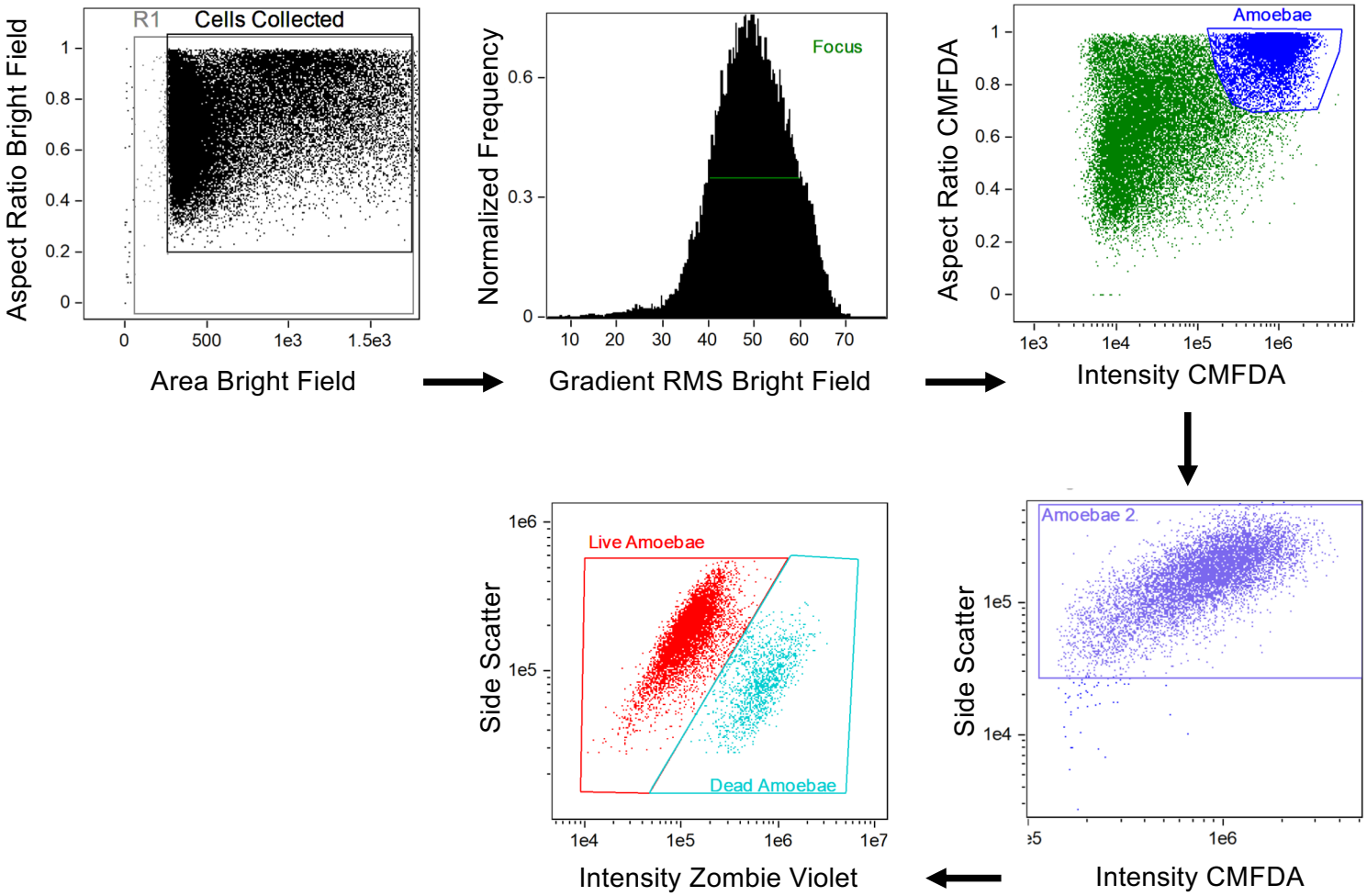
R1
Cells Collected
Aspect Ratio Bright Field
Area Bright Field
Normalized Frequency
Focus
Gradient RMS Bright Field
Aspect Ratio CMFDA
Amoebae
Intensity CMFDA
Side Scatter
Amoebae 2
Intensity CMFDA
Side Scatter
Live Amoebae
Dead Amoebae
Intensity Zombie Violet